

CORRELATION OF RPOB GENE MUTATION WITH  
CLINICAL RIFABUTIN AND RIFAMPICIN RESISTANCE FOR TREATMENT OF  
CROHN'S DISEASE

by

DANIEL RYAN BECKLER  
B.S. University of Central Florida, 2005

A thesis submitted in partial fulfillment of the requirements  
for the degree of Master of Science  
in the Department of Molecular Biology and Microbiology  
in the Burnett College of Biomedical Sciences  
at the University of Central Florida  
Orlando, Florida

Summer Term  
2007

Major Professor: Saleh Naser

© 2007 Daniel Ryan Beckler

## ABSTRACT

Emerging rise in microbial drug resistance and the slow-growing characteristic of some intracellular pathogens such as MAP (*Mycobacterium avium subspecies paratuberculosis*) strongly urges the need for an effective approach for unconventional drug susceptibility testing. We designed a molecular-based PCR method for the evaluation of rifabutin (RFB) and rifampicin (RIF) resistance based on probable determinant regions within the *rpoB* gene of MAP, including the 81 bp variable site located between nucleotides 1363 and 1443. The minimum inhibitory concentration (MIC) for RIF was also determined against 10 MAP isolates in attempt to seek correlation with *rpoB* sequences. We determined that MAP strain 18 had an MIC > 30 ug/ml and  $\geq 5$  ug/ml for RIF and RFB respectively, and a significant *rpoB* mutation C1367T, compared to an MIC of  $\leq 1.0$  ug/ml for both drugs in the wild type MAP. The 30-fold increase in the MIC was a direct result of the *rpoB* mutation C1367T, which caused an amino acid change Thr456 to Ile456 in the drug's binding site; the beta subunit of RNA polymerase. Our in vitro induced mutation in MAP strain UCF5 resulted in the generation of a new resistant strain (UCF5-RIF16r) that possessed T1442C *rpoB* mutation and an MIC > 30 ug/ml and > 10 ug/ml for RIF and RFB respectively. The T1442C mutation resulted in a Leu481 to Pro481 amino acid change, consequently altering the beta subunit sequence. Sequencing the entire 3.5 kb *rpoB* in strains 18 and UCF5-RIF16r revealed no additional expressed nucleotide mutation.

Of the 10 MAP strains analyzed, an additional one strain (UCF4) exhibited a slight increase in the MIC against RIF and RFB compared to the wild-type. Nucleotide

sequencing of the *rpoB* gene revealed an A2284C mutation in strain UCF4 that occurred further downstream of the expected probable *rpoB* region and resulted in an amino acid alteration Asn762 to His762. The location of this mutation outside the binding site and its correlation with the minor increase in MIC suggests a possible secondary interaction between the drug and the beta subunit.

We have provided three dimensional images through the utilization of PyMol Molecular-based Graphics to display a clear comparison of the mutations observed in the beta subunit for MAP strains 18, UCF5-RIF16r, and UCF4. We propose that these alterations may have caused a less stable interaction between RIF and the beta subunit, resulting in the observed increased in MIC. Furthermore, the change in amino acid sequence did not affect the viability for our RIF resistant strains.

The data clearly illustrates that clinical and in vitro-induced MAP mutants with *rpoB* mutations result in resistance to RIF and RFB. Consequently, unconventional drug susceptibility testing such as our molecular approach will be beneficial for evaluation of antibiotic effectiveness. This molecular approach may also serve as a model for other drugs used for treatment of MAP infections.

The following thesis is dedicated to my family, for providing me with the love and support that made my academic progress possible.

## **ACKNOWLEDGEMENTS**

I thank Dr. Saleh Naser for his guidance and education, and for the opportunity to conduct research in a laboratory devoted to Crohn's Disease. In addition, my thanks are due to Dr. Pappachan E. Kolattukudy, Dr. Henry Daniell, and Dr. Kenneth Teter for contributing their knowledge and serving as part of my graduate committee. I also extend thanks to Dr. George Ghobrial, Mounir Chehtane, Kit Fuhrman, Dr. Kathleen Nemec and Charalambos Kaittanis for their technical assistance. I thank my family for their love, guidance, and support. Jessica, thank you for providing me with love, friendship and support, and everyone else that contributed to my progress throughout graduate school. Your support has made my success possible.

# TABLE OF CONTENTS

LIST OF FIGURES.....	ix
LIST OF TABLES.....	xi
1. INTRODUCTION.....	1
1.1. Crohn’s Disease and MAP.....	1
1.2. Rifabutin and Rifampicin.....	1
1.3. rpoB and Rifamycin Resistance.....	2
1.4. Rifabutin and Crohn’s Disease .....	2
1.5. Fastidious MAP .....	2
1.6. Research Objective .....	3
2. MATERIALS AND METHODS .....	4
2.1. Bacterial Strains .....	4
2.2. Growth Conditions .....	4
2.3. Minimum Inhibitory Concentration (MIC) .....	7
2.4. DNA Extraction .....	7
2.5. Nested PCR.....	9
2.6. rpoB PCR .....	9
2.7. PCR Purification .....	10
2.8. Nucleotide Sequencing.....	10
2.9. BLAST .....	11
2.10. In-Vitro Mutant .....	11
2.11. PyMOL Images.....	12
3. RESULTS.....	13
3.1. IS900 Verification.....	13

3.2. rpoB PCR .....	16
3.3. rpoB Sequencing .....	17
3.4. Susceptibility.....	22
3.5. UCF5-RIF16r .....	24
3.6. Blood Mixture.....	25
3.7. Taq Alignment .....	25
3.8. 3-D perspective .....	28
3.8.1    MAP strain 18 3-D model.....	28
3.8.2    UCF5-RIF16r 3-D model.....	31
3.8.3    Proposition.....	31
3.9. Additional Sequencing .....	35
3.10. UCF4 3-D model.....	40
3.11. Entire rpoB Sequence.....	43
4. DISCUSSION .....	52
4.1. Purpose .....	52
4.2. Rationale .....	52
4.3. An alternative approach.....	53
4.4. Molecular analysis .....	54
4.5. Induced resistance.....	54
4.6. Blood mixture.....	54
4.7. Final Comments .....	55
REFERENCES.....	56



## LIST OF FIGURES

Figure 1 IS900-based PCR for detection of MAP using P90/P91 primers.....	13
Figure 2 IS900-based PCR for detection of MAP using AV1/AV2 primers.....	14
Figure 3 Partial rpoB amplicons produced by PCR. ....	16
Figure 4 Sequence alignment of the 81 base pair region in the rpoB gene of MAP. ....	19
Figure 5 Characterization of MAP isolates. ....	20
Figure 6 Percent inhibition at 1 ug/ml of RIF for each bacterial sample. ....	23
Figure 7 Minimum Inhibitory Concentration (MIC) for each bacterial sample. ....	23
Figure 8 Sequence alignment of MAP with <i>Thermus aquaticus</i> and <i>Mycobacterium tuberculosis</i> . ....	27
Figure 9 <i>Thermus aquaticus</i> RIF complex model for MAP wildtype. ....	29
Figure 10 <i>Thermus aquaticus</i> RIF complex for resistant MAP strain 18.....	30
Figure 11 <i>Thermus aquaticus</i> RIF complex for wildtype MAP strain UCF5.....	32
Figure 12 <i>Thermus aquaticus</i> RIF complex for resistant MAP strain UCF-RIF16r. ....	33
Figure 13 Interactions with RIF and RNA polymerase.....	34
Figure 14 rpoB PCR results using Efox1/Fox1r primers.....	37
Figure 15 rpoB PCR results using Fox1/DBR primers.....	37
Figure 16 rpoB PCR results using Ex1a/Ex2a primers.....	38
Figure 17 rpoB PCR results using Ex3/Ex4 primers.....	38
Figure 18 rpoB PCR results using Ex5/Hrox1 primers. ....	39
Figure 19 <i>Thermus aquaticus</i> RIF complex for wild-type MAP.....	41
Figure 20 <i>Thermus aquaticus</i> RIF complex for MAP strain UCF4.....	42

Figure 21 Entire rpoB gene sequence for MAP strain K-10, wild-type control sequence  
(Li et al 2005). ..... 45

Figure 22 Entire rpoB gene sequence for MAP strain M18. .... 47

Figure 23 Entire rpoB sequence for induced MAP strain UCF5-RIF16r. .... 49

Figure 24 Entire rpoB sequence for MAP strain UCF4. .... 51

## LIST OF TABLES

Table 1 List of microorganisms used in the study. ....	6
Table 2 PCR primers used in this study. ....	15
Table 3 rpoB and susceptibility data for all microorganisms.....	21
Table 4 Additional rpoB PCR primers.....	36

# 1. INTRODUCTION

## 1.1. Crohn's Disease and MAP

Crohn's disease (CD) is an inflammatory bowel disease that detrimentally affects the epithelial lining of the digestive tract and includes symptoms such as diarrhea, weight loss, abdominal pain, and constipation (12). The disease's symptoms are similar to that of the inflammatory intestinal disease found in cattle, Johne's disease (JD) (12). Currently a strong debate exists between CD's potential autoimmune cause and its relation to bacteria, and either concept has yet to be proven. *Mycobacterium avium subspecies. paratuberculosis*, or MAP, is known to be the causative agent of Johne's disease and has previously been implicated in etiological studies of CD (10,11,16). Available information regarding MAP's role in CD has enabled ongoing studies to further conclude the relationship between the bacteria and the human disease (5,6,9,10,11,13,16,20,21,22,31,32,35,36,38). Evidence has shown that an insertion sequence known as IS900 is unique to MAP, and a nested PCR reaction that amplifies this region enables the detection of the bacteria in CD samples of blood and tissue, and also pasteurized milk (14,31,35).

## 1.2. Rifabutin and Rifampicin

Rifabutin (RFB) and rifampicin (RIF) are antibiotics that belong to the rifamycin drug family and are very similar in chemical structure. The function of these antibiotics are to inhibit the growth of bacteria, specifically by binding to the beta subunit of RNA polymerase through direct and indirect amino acid interactions, and preventing the production of nascent RNA transcripts (7).

### **1.3. rpoB and Rifamycin Resistance**

The rpoB gene in prokaryotes encodes the beta subunit, and it is known that mutations within this gene result in a higher level of resistance to the rifamycin antibiotics in several bacteria (15,18,25,27,30,33). Moreover, mutations within an 81 base pair region in rpoB spanning nucleotides 1276-1356 in *Mycobacterium tuberculosis* has shown to contain the majority of alterations relating to rifamycin resistance (34). In addition, the V176F mutation in the beginning of rpoB has been associated with rifamycin resistance in some strains of *M. tuberculosis*, however this alteration is not as prevalent as the former (18,19).

### **1.4. Rifabutin and Crohn's Disease**

Previous reports have shown that RFB may potentially serve as a therapeutic agent for the treatment of CD (17,36). As a result, more attention has been focused on the possible use of antibiotics as an alternative remedy. However, a screening method for RIF and RFB resistant strains of MAP has yet to be established. Therefore, as CD therapy becomes more focused on antibiotics, it is essential that a method for susceptibility testing be developed in order to detect and monitor MAP strains for RIF and RFB resistance.

### **1.5. Fastidious MAP**

Unlike other prokaryotes, MAP is very fastidious and requires unusual in vitro growth conditions, including the addition of Mycobactin J. Additionally, MAP cultured from CD samples has shown to lack a cell wall, and this characteristic is a major contributing factor to the complexity of the bacteria's primary isolation process (23,31,32). Consequently, conventional drug susceptibility tests involving MAP are not reliable and may result in inaccurate measurements. Therefore, the challenges faced

when working with this bacterium must be counteracted via alternate approaches that could potentially result in the exposition of significant data in order to effectively treat MAP infections.

### **1.6. Research Objective**

In this study, we execute a molecular approach based on PCR amplification, followed by nucleotide sequencing of regions within the rpoB gene of MAP. We attempt to investigate and identify regions of the rpoB gene that exhibit expressed mutation and to seek correlation between rpoB mutations in clinical MAP strains with susceptibility to RIF and RFB.

## 2. MATERIALS AND METHODS

### 2.1. Bacterial Strains

Bacterial isolates investigated in this study are listed in Table 1. All clinical strains including UCF3, UCF4, UCF5, UCF7, UCF8, M18, M185, and 61a were isolated in our laboratory from clinical samples obtained from CD patients (37). Cow2013, and Cow5 MAP strains were recently isolated from ground beef samples from two cattle with Johne's disease. In addition, the MAP strains used in our study were previously isolated from CD patients and JD cows, and were maintained in culture medium for long-term use (Table 1).

### 2.2. Growth Conditions

Briefly, tissue samples were homogenized, decontaminated and then inoculated into MGIT culture media with supplements including OADC, Mycobactin J and PANTA as described previously (37). Prior to inoculation, each BBL MGIT 4 mL tube (Becton Dickinson cat #245111) was supplemented with 500  $\mu$ L MGIT oleic acid-albumin-dextrose-citrate (OADC) (Becton Dickinson cat # 245116), 100  $\mu$ L antibiotic mixture (200 U Polymyxin B, 287 mcg amphotericin B, 274 mcg nalidixic acid, 20 mcg trimethoprim, and 20 mcg azlocillin (PANTA) (Becton Dickinson cat # 245114 ), 8  $\mu$ L Mycobactin J (0.5 mg/mL) (Allied Monitor, USA) and sucrose to a final concentration of 0.1%. Each MGIT was then inoculated with 500  $\mu$ L of the homogenized sediment suspension using 1 mL sterile syringe with a BD 18G 1½ needle. After contents were mixed well, MGITs were incubated at 37° C in a 5% CO<sub>2</sub>. The MGIT tubes were monitored weekly for visible turbidity or an increase in fluorescence quenching by exposing the tubes to UV light at 365 nm.

All ATCC strains were purchased from ATCC and verified in our laboratory by biochemical and molecular testing. All cultures were subcultured in 7H10 agar supplemented with OADC and mycobactin J. Plates were incubated at 37°C until visible colonies were observed. Colonies from pure culture verified by Ziel-Neelson acid fast stain and IS900-based PCR for MAP were used to inoculate BACTEC 7H9 broth culture supplemented with 500 uL OADC and 2.4 uM Mycobactin J. Growth index (G.I.) was read weekly until optimum growth of desired G.I. was observed. The fresh culture was then used for drug susceptibility testing and for molecular studies.



**Table 1 List of microorganisms used in the study.**

Microorganism	Strain	Source
MAP	43544	ATCC
MAP	UCF3, Clinical Isolate	CD, Ileal
MAP	UCF4, Clinical Isolate	CD, Ileal
MAP	UCF5, Clinical Isolate	CD, Ileocolonic
MAP	UCF7, Clinical Isolate	CD, Ileocolonic
MAP	UCF8, Clinical Isolate	CD, Ileal
MAP	18, Clinical Isolate	CD, Ileal
MAP	185, Clinical Isolate	CD, mesenteric lymphnode
MAP	61a, Clinical Isolate	CD, Ileal
MAP	Cow2013	JD, ground beef
MAP	Cow5	JD, ground beef
<i>M. avium subspecies.</i> <i>avium</i>	25291	ATCC
<i>M. tuberculosis</i>	Ra25177	ATCC
<i>M. smegmatis</i>	607	ATCC

### 2.3. Minimum Inhibitory Concentration (MIC)

MIC for RIF and RFB were determined against microorganisms listed in Table 1 as follows. Starting cultures with a G.I. in the range of 500-600 were determined to be best for inoculation. The inoculum size for each Bactec bottle used in the drug susceptibility study was approximately  $1.0 \times 10^5$  CFUs. Serial dilutions of RIF concentration ranging from 0.0 to 4 ug/ml were evaluated against all microorganisms. MAP strains resistant to RIF > 1.0 ug/ml were further tested against RIF concentrations of 10, 20 and 30 ug/mL for MIC measurement. These MAP strains were also evaluated against RFB at concentrations ranging from 0.0 to 10 ug/mL, excluding UCF4. MAP wild type was included as a control in every batch of analysis. Experiments were repeated for confirmations. Microorganisms other than MAP were also evaluated for RIF concentrations ranging from 0.0 to 10.0 ug/mL. The percentage of RIF or RFB inhibition was used to determine the level of susceptibility for each concentration of antibiotic as follows: % Inhibition =  $1 - \frac{\text{G.I of Bactec culture}_{\text{without drug}} - \text{G.I of Bactec culture}_{\text{with drug}}}{\text{G.I of Bactec culture}_{\text{without drug}}}$ . The MIC was also determined for each bacterial sample, and was defined as the minimum concentration of antibiotic that induced 90% inhibition of growth.

### 2.4. DNA Extraction

Extraction of genomic DNA from mycobacterial isolates was performed for verification of the presence of the IS900 gene and for analysis of rpoB gene sequence. For extraction of genomic DNA from *Mycobacterium paratuberculosis*, the boiling method with the use of Phase-Lock Gel tubes, PLG (Eppendorf 0032005-101) gave excellent results. The procedures for this method are summarized as follows: Before sampling,

incubated MGIT tubes were thoroughly vortexed. Sample of 500 $\mu$ L was aseptically taken from each MGIT cultures, using a sterile disposable 1 mL syringe with a long sterile needle BD 18G 1 $\frac{1}{2}$ , and placed into a 1.5 mL sterile eppendorf tubes. Tubes were centrifuged at 12,000 rpm for 10 minutes at 4° C. Supernatants were removed; using micropipeter with aerosol barrier tips, into an autoclavable container containing 30 mL bleach. Pellets, containing mycobacterial cells, were re-suspended in 100  $\mu$ L sterile TE buffer (10 mM Tris and 1 mM EDTA, pH 8.0 HCl). The tubes were incubated in a dry heat bath at 100° C for 30 minutes, thereafter placed on ice for 15 minutes.

Immediately prior to use, Phase-Lock Gel tubes, PLG, 2-mL light (Eppendorf cat # 0032 005 101) were pelleted in a microcentrifuge at 12,000 rpm for 20 seconds at 4° C.. The tubes containing DNA were centrifuged at 12,000 rpm for 10 minutes at 4° C. Supernatants were transferred into the Phase Lock Gel tubes using a micro micropipette with sterile aerosol-barrier tips. Then, 200  $\mu$ L of phenol / chloroform / iso amayl alcohol (Acros Organics, cat # 327115000) was added to each PLG tube, thoroughly mixed with the aqueous sample to form a transiently homogeneous suspension.. The PLG tubes were then centrifuged at 12,000 rpm for 5 minutes at 4° C. The gel of PLG formed a barrier between the aqueous and organic phases. The aqueous upper phase containing DNA was carefully transferred to a fresh 1.5 mL eppendorf sterile tube using sterile aerosol-barrier tips. To precipitate extracted DNA, 400  $\mu$ L of 100% ethanol cooled to -20° C was added to each tube, mixed well, then tubes were incubated at -20 C overnight. Tubes were centrifuged at 14,000 rpm for 20 minutes at 4° C. Supernatants were removed and DNA pellets were washed with 400  $\mu$ L of 80% ethanol. Tubes were re-centrifuged at 14,000 rpm for 20 minutes at 4° C.

Supernatants were removed and DNA pellets were dried in a speed vacuum for 10 minute at room temperature. Finally, 50 µL of sterile millipore water was added to each dried DNA pellet and allowed to re-dissolve at 4°C overnight.

## **2.5. Nested PCR**

Nested PCR for IS900 amplification was performed using the primers p90/91 and AV1/AV2 (Table 2) as described previously (31). The amplification product size was determined on 2% agarose gel. Appropriate negative controls for PCR consisted of sterile TE buffer or sterile water in place of the DNA template were used in parallel with each round of PCR preparation. Positive MAP DNA from strain ATCC 43015 was prepared independently and added to PCR tubes at a different facility using separate supplies.

## **2.6. rpoB PCR**

Unlike the nested IS900-based PCR assay, only one round of PCR assays were developed for amplification of two different regions of the rpoB gene. Therefore, one PCR reaction contained the UCF1/UCF2 primers for an amplification of 448 bp where as the second PCR reaction contained the Knight1/Knight 2 primers for an amplification of 587 bp. For polymerase chain reaction, the following reagents were added in respective order in a 500-µL sterile PCR tube: 12.30 µL of Millipore sterile, filtered and autoclaved water, 5.00 µL of 10x Platinum Taq polymerase buffer with MgCl<sub>2</sub> (Invitrogen), 6.00 µL 25mM Magnesium solution (Invitrogen), 8.50 µL of 3M Betaine (ICN 101003), 1.00 µL of 10 mM each PCR Nucleotide Mix dNTP (Fisher Bp2565-2), 1.00 µL of either forward primer UCF1 (5'TCGATGTCGCTGTCTTTCTC) or Knight1 (5'ACCACTTCGGCAACCGCCGG) at a concentration of 0.125 µg/µL, 1.00 µL of either reverse primer UCF2 (5' GCTCGGTGATCTGCTCGTTG) or Knight2 (5'ACTCGACCTCGCCCGCCTTG) at a

concentration of 0.125 µg/µL, 0.20 µL of Platinum Taq DNA Polymerase (Invitrogen), and 15.00 µL of extracted DNA (Template) 0.3 – 3.0 ng/µL, making a total of 50.00 µL per 0.5 µL PCR tube. Table 2 lists the nucleotide sequence for all primers used in this study.

Additional PCR was performed for MAP strains UCF4, M18, and UCF5-RIF16r using the same protocol as previously described. Table 4 displays information regarding additional rpoB primers and the corresponding regions that each primer set amplifies.

## **2.7. PCR Purification**

Each rpoB PCR product was purified from agarose using the Purelink™ Quick Gel Extraction Kit following the procedure as described by the manufacturer (Invitrogen™). Purified DNA was then quantitated and subjected to nucleotide sequencing.

## **2.8. Nucleotide Sequencing**

Sequencing was performed using the GenomeLab™ DTCS – Quick Start Kit following the procedure as described by the manufacturer (Beckman Coulter®). Each sequencing reaction contained the following reagents their corresponding range of volumes: 0 – 9.5 ul dionized H<sub>2</sub>O, 0.5 – 10 ul DNA (PCR) template, 2.0 ul primer (forward or reverse), and 8 ul DTCS Quick Start Master Mix totaling 20 ul. The thermal cycling protocol consisted of 30 cycles using the following times and temperatures: 96°C for 20 seconds, 50°C for 20 seconds, and 60°C for 4 minutes. Sequenced DNA was then precipitated in individual tubes using the following protocol: a) Prepare a labeled, sterile 0.5 ml microfuge tube for each sample, b) Prepare fresh Stop Solution/Glycogen mixture as follows (per sequencing reaction): 2 ul of 3M Sodium Acetate (pH5.2), 2 uL of 100 mM Na<sub>2</sub>-EDTA (pH 8.0) and 1 ul of 20 mg/mL of glycogen.

To each of the labeled tubes, add 5 uL of the Stop Solution/Glycogen mixture, c) Transfer the sequencing reaction to the appropriately labeled 0.5 mL microfuge tube and mix thoroughly, d) Add 60 uL cold 95% (v/v) ethanol/dH<sub>2</sub>O from -20°C freezer and mix thoroughly. Immediately centrifuge at 14,000 rpm at 4°C for 15 minutes. Carefully remove the supernatant with a micropipette (the pellet should be visible), e) Rinse the pellet 2 times with 200 ul 70% (v/v) ethanol/dH<sub>2</sub>O from -20°C freezer. For each rinse, centrifuge immediately at 14,000 rpm at 4°C for a minimum of 2 minutes. After centrifugation carefully remove all of the supernatant with a micropipette, f) Vacuum dry for 10 minutes (or until dry), g) Resuspend the sample in 40 ul of the Sample Loading Solution (provided with kit). Following the sequencing reaction, capillary electrophoresis was performed using the appropriate nucleotide primers for both strands of the PCR product at the Biomolecular Science Center DNA Sequencing Core facility at the University of Central Florida.

## **2.9. BLAST**

BLAST and alignment sequence analyses was performed using [www.ncbi.nlm.nih.gov](http://www.ncbi.nlm.nih.gov). Briefly, sequences were obtained from the ftp://name@10.169.1.31 database available through the Burnett College of Biomedical Sciences at the University of Central Florida. Sequences were used to align and BLAST against the wildtype K-10 MAP strain available on pubmed.gov. Both forward and reverse reactions were analyzed for mismatches and sequences were reported for each MAP isolate accordingly.

## **2.10. In-Vitro Mutant**

A RIF resistant MAP mutant (UCF5-RIF16r) was generated through the induction of an rpoB mutation. This was performed by exposing a wild-type MAP strain UCF5 to

increasing concentrations of RIF ranging from 1 to 16 ug/ml. Initially, MAP strain UCF5 was inoculated into a BACTEC bottle containing 1 ug/ml of RIF. Following incubation, surviving MAP cells were subcultured into a new BACTEC bottle with double RIF concentration. The process was repeated several times until a new MAP strain (UCF5-RIF16r) was generated that was able to survive in the presence of 16 ug/ml of RIF. This new resistant strain was then tested for MIC against RIF and RFB and investigated for possible rpoB mutations as described earlier.

### **2.11. PyMOL Images**

Protein database (pdb) file 1Ynn was obtained from the RCSB Protein Data Bank [www.rcsb.org/pdb/home/home.do](http://www.rcsb.org/pdb/home/home.do) website, and docking images were provided through the use of DeLano, W.L. MacPyMOL: A PyMOL-based Molecular Graphics Application for MacOS X (2005). Mutagenesis was displayed through using the Mutatgenesis option in MacPyMOL.

### 3. RESULTS

#### 3.1. IS900 Verification

Genomic DNA from all bacterial isolates was subjected to IS900-based PCR in order to confirm the identity of the MAP strains listed in Table 1. This procedure involved two rounds of PCR, using p90/91 primers in the first round to amplify a 400 bp sequence (Fig 1). The use of AV1/AV2 in the second round of PCR amplified a 308 bp sequence and provided exceptional sensitivity and enhanced specificity for the confirmation of MAP. All 10 MAP isolates were confirmed for the presence of IS900 (Fig 2, lanes 1-11). As expected, *M. avium* subspecies *avium*, *M. smegmatis* and *M. tuberculosis* displayed negative results for the presence of the IS900 (Fig 2, lanes 12-14). Succeeding the IS900 PCR analysis, genomic DNA from each identified MAP strain was then used as template for PCR employing rpoB primers (Table 2).

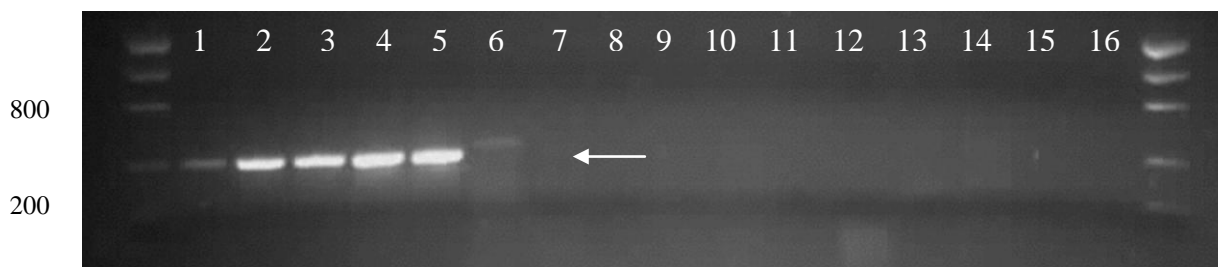


**Figure 1 IS900-based PCR for detection of MAP using P90/P91 primers.**

This first round of the nested PCR using P90/P91 primers generated a 400 bp sequence displayed on 2% agarose gel. Lanes 1-16 correspond to the following: 1, MAP strain 43544 (positive control); 2, UCF3; 3, UCF4; 4, UCF5; 5, UCF7; 6, UCF8; 7, M18; 8, MAP185; 9, Cow2013; 10, Cow5; 11, 61a; 12, *M. avium*; 13, *M. tuberculosis*; 14, *M. smegmatis*, 15, TE buffer; 16, negative control.



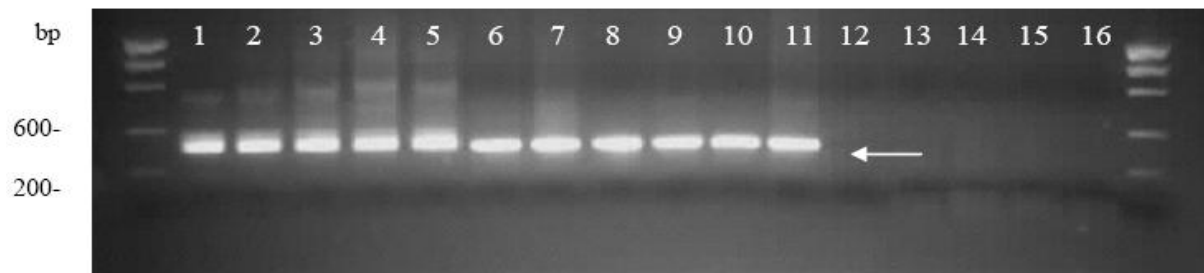


**Figure 2 IS900-based PCR for detection of MAP using AV1/AV2 primers.**

This second round of the nested PCR using AV1/AV2 primers generated a 308 bp on 2% agarose gel. Lanes 1-8 correspond to MAP strains isolated from human tissue samples (1, MAP strain 43544 (control); 2, UCF3; 3, UCF4; 4, UCF5; 5, UCF7; 6, UCF8; 7, MAP18; and 8, MAP185; respectively). Lanes 9 and 10 correspond MAP strains derived from cattle tissue (strains Cow2013 and Cow5, respectively). Lane 11 corresponds to a new MAP strain 61a from human tissue. Lanes 12-14 correspond to *M. avium* subspecies *avium*, *M. tuberculosis* and *M. smegmatis*, respectively. Lanes 15 and 16 correspond to negative control for DNA extraction and PCR, respectively. A low mass DNA molecular weight marker was used and bp are indicated on the left of the diagram.

**Table 2 PCR primers used in this study.**

Primer Type and Name	Sequence (5' to 3')	Amplified Base Pairs (bp)*	Amplicon Length (bp)
IS900			
P90	GTTTCGGGGCCGTCGCTTAGG	22-421	400
P91	GAGGTCGATCGCCCACGTGA		
AV1	ATGTGGTTGCTGTGTTGGATGG	77-384	308
AV2	CCGCCGCAATCAACTCCAG		
rpoB			
UCF1	TCGATGTCGCTGTCTTTCTC	373-820	448
UCF2	GCTCGGTGATCTGCTCGTTG		
Knight1	ACCACTTCGGCAACCGCCGG	1191-1777	587
Knight2	ACTCGACCTCGCCCGCCTTG		

\*Numbers represent nucleotide positions within the rpoB gene of MAP.

### 3.2. rpoB PCR

Amplification of rpoB sequences enabled the possibility for amplicon purification, sequencing, and subsequently BLAST analysis. The use of primers UCF1/UCF2 and Knight1/Knight2 enabled the amplification of two regions of the rpoB gene of MAP. These regions overlapped similar sequences in the rpoB gene of *M. tuberculosis* previously associated with rifamycin resistance. Moreover, PCR with Knight1/Knight2 primers amplified a sequence that harbored the 81 bp variable site 1363-1443, a highly probable determinant region for rifamycin resistance in closely related bacteria. Figure 3 shows the PCR results of these two regions of the rpoB gene from each of five MAP strain representatives.

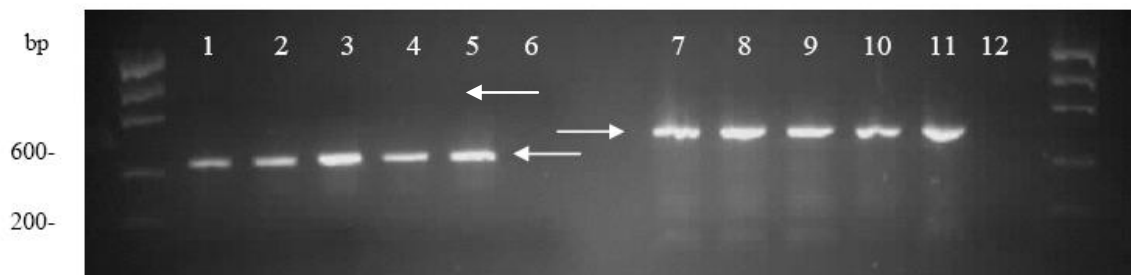


**Figure 3 Partial rpoB amplicons produced by PCR.**

These five samples including the positive control were chosen to represent the results of rpoB PCR for all MAP strains in this study. Lanes 1-6 represent PCR using primers UCF1/UCF2, and each lane corresponds to a 448 bp amplicon and is associated with the following MAP strains: 1, 43544 (positive control); 2, UCF4; 3, UCF5; 4, MAP18; 5, MAP185; 6, negative control. Lanes 7-12 represent PCR using primers Knight1/Knight2, and each lane corresponds to a 587 base pair amplicon and is associated with the following MAP strains: 7, 43544 (positive control); 8, UCF4; 9, UCF5; 10, MAP18; 11, MAP185; 12, negative control. A low mass DNA marker was used and the numbers located on both sides of the image indicate base pair lengths for two different bands within the marker. Arrows indicate location of partial rpoB DNA fragments.

### 3.3. rpoB Sequencing

Nucleotide sequencing of regions amplified by primers UCF1/UCF2 and Knight1/Knight2 for all MAP strains was performed using a High Fidelity Platinum® Taq polymerase. The process was repeated and the sequence was verified with both forward and reverse primer reactions to exclude any possible errors in the data. Therefore, sequence data was reported as completely accurate upon the confirmation of error-free reactions. We investigated the regions amplified by primers UCF1/UCF2 and Knight1/Knight2 in 10 MAP strains, which resulted in the detection of either identical (wild-type) or non-identical sequences (Table 3). MAP strains consisting of the latter were further detected for silent mutations with no effect on amino acid expression, or mutations that differentially expressed the amino acid sequence of the beta subunit. The location of each changed amino acid was then identified and determined to lie within the 81 bp region contained in the sequence amplified by primers Knight1/Knight2 (Fig 4).

Of the 10 MAP clinical isolates, 9 (90%) consisted of no rpoB mutation in the two regions investigated, however, 1 (10%) MAP strain, M18, possessed two rpoB mutations, and these included C1367T and T1375C (Fig 4). The C1367T mutation resulted in a significant amino acid change from Thr456 to Ile456 in the beta subunit of RNA polymerase (Fig 4, Table 3). This amino acid change was considered indicative of RIF and RFB resistance, which later was verified through susceptibility tests. The T1375C mutation had no effect on the beta subunit, and was therefore characterized as silent (Fig 4, Table 3). MAP isolates were then classified based on sequence information from both regions (Fig 5). Isolates that contained no mutations were termed wild-type and were classified as identical compared to the K-10 sequence rpoB

sequence. Consequently, isolates that possessed mutations were classified as non-identical. The effect of *rpoB* mutations in these regions on RIF and RFB susceptibility were investigated following sequence analysis.



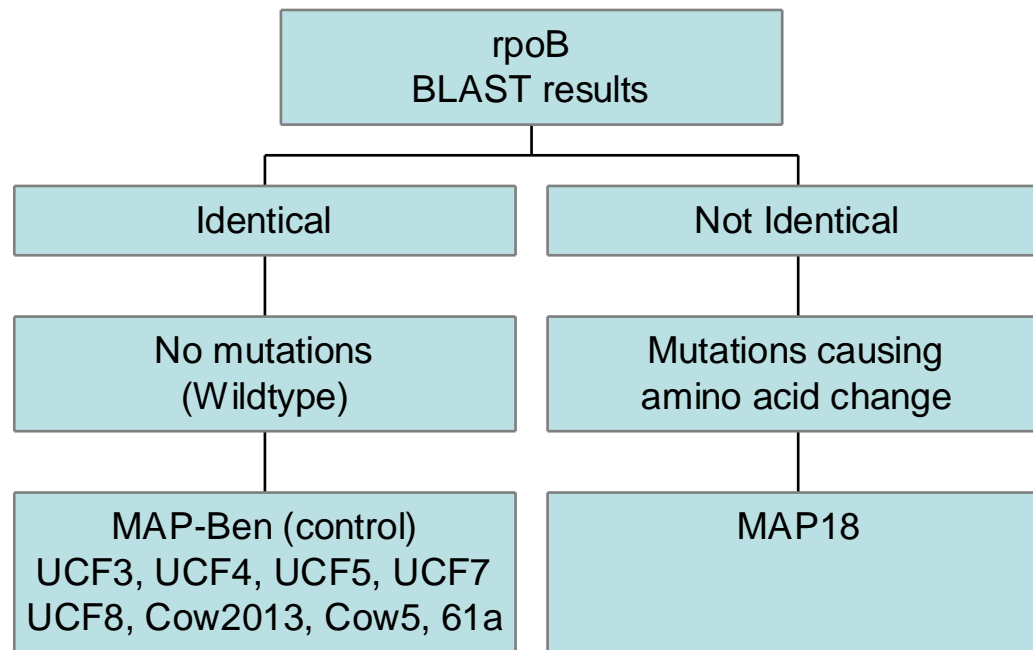


**Figure 5 Characterization of MAP isolates.**

According to *rpoB* sequence information regarding regions amplified by primers UCF1/UCF2 and Knight1/Knight2, one of the ten MAP isolates contained mutations, and was therefore characterized as non-identical.

**Table 3 rpoB and susceptibility data for all microorganisms.**

Microorganism	Strain	RIF MIC (ug/ml)	RFB MIC (ug/ml) <sup>a</sup>	Inhib. at 1 ug/ml of RIF (%) <sup>b</sup>	rpoB BLAST result <sup>c</sup>	Amino acid change <sup>d</sup>
MAP	ATCC43544	≤ 1.0	≤ 1.0	91 ± 0.71	WT	None
MAP	UCF3	≤ 1.0	n/a	94 ± 2.83	WT	None
<b>MAP</b>	<b>UCF4</b>	<b>≤ 2.5</b>	<b>n/a</b>	<b>79 ± 7.07</b>	<b>A2284C</b>	<b>N762H</b>
MAP	UCF5	≤ 1.0	n/a	92.5 ± 0.71	WT	None
MAP	UCF7	≤ 1.0	n/a	88 ± 5,66	WT	None
MAP	UCF8	≤ 1.0	n/a	90 ± 1.41	WT	None
<b>MAP</b>	<b>18</b>	<b>≥ 30</b>	<b>≤ 5.0</b>	<b>42 ± 1.00</b>	<b>1, C1367T; 2, T1375C</b>	<b>1, T456I; 2, silent</b>
MAP	Cow2013	≤ 1.0	n/a	95 ± 1.41	WT	None
MAP	Cow5	≤ 1.0	n/a	96.5 ± 0.71	WT	None
MAP	61a	≤ 1.0	n/a	90 ± 3.54	WT	None
<i>M. avium</i> subspecies. <i>avium</i> <sup>e</sup>	ATCC25291	≤ 1.0	n/a	90 ± 1.41	n/a	n/a
<i>M. tuberculosis</i> <sup>e</sup>	ATCC25177	≤ 1.0	n/a	92 ± 1.41	n/a	n/a
<i>M. smegmatis</i> <sup>e</sup>	ATCC607	≥ 9.0	n/a	6.6 ± 1.7	n/a	n/a
<b>UCF5-RIF16r</b>	<b>Modified UCF5</b>	<b>≥ 30</b>	<b>≥ 10</b>	<b>32 ± 1.41</b>	<b>T1442C</b>	<b>L481P</b>

a. Limited investigation involving MAP18, and UCF5-RIF16r.

b. Values are expressed as means ± the standard deviation (SD).

c. Wildtype (WT) indicates identical investigated rpoB sequence compared to MAP K-10 strain.

d. The amino acid change is indicated with single letter amino acid codes and the corresponding codon number.

e. rpoB sequence was not investigated



### 3.4. Susceptibility

Correlation between *rpoB* sequence analysis and inhibitory growth rates for RIF was assessed for all 10 MAP strains. MAP strains were initially tested against 1 ug/ml of RIF, the MIC for our control (Fig 6). MAP strains were then subjected to MIC tests against the same drug (Fig 7). All strains clearly indicated a susceptible characteristic by ceasing growth at 1ug/ml of RIF, the MIC of our wild-type control, except UCF4, M18, and UCF5-RIF16r (UCF5-RIF16r explained in later sections). More specifically, 9 MAP strains including ATCC43544 (control), UCF3-5, UCF7-8, 61a, Cow2013, Cow5, and two non-MAP controls including *M. tuberculosis* and *M. avium* subspecies *avium* had an MIC  $\leq 1.0$  ug/mL for RIF (Fig 7, Table 3). After analyzing our susceptibility results (Fig 6, Fig 7), MAP strains displaying suspicious characteristics of RIF resistance were then subjected to a susceptibility test against RFB (Table 3). Only MAP strain M18 displayed growth of up to 5 ug/ml of RFB, indicating partial resistance to this drug as well. The MIC for RIF of the remaining MAP strains 18, UCF4, and *M. smegmatis* was determined as  $\geq 30$ ,  $\leq 2.5$ ,  $\geq 9$  ug/ml respectively (Table 3). Despite the lack of *rpoB* mutations, *M. smegmatis* is commonly characterized as a naturally RIF resistant bacteria. Table 3 summarizes *rpoB* mutations and susceptibility test values for all microorganisms analyzed in this study.

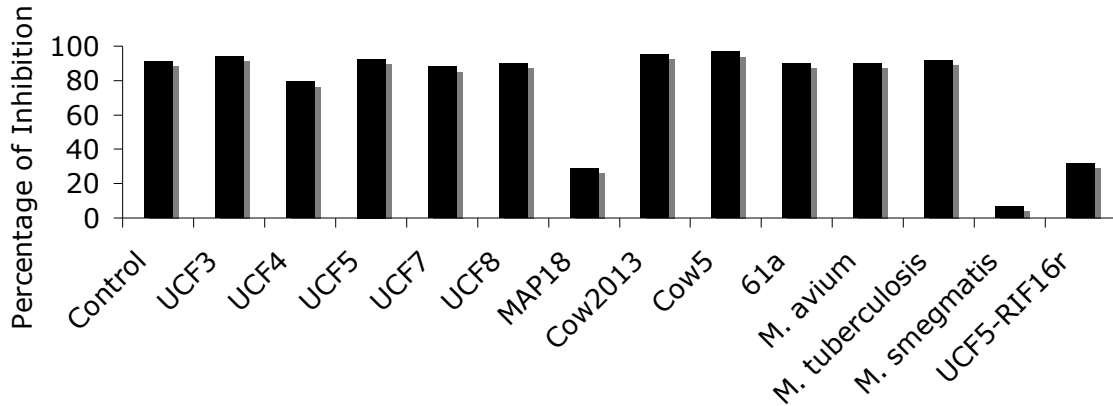


**Figure 6 Percent inhibition at 1 ug/ml of RIF for each bacterial sample.**

The y-axis represents inhibition of growth expressed as a percentage. The x-axis represents all bacterial isolates tested. The growth rate of MAP18, UCF4, MAP185, M. smegmatis and UCF5-RIF16r was not affected as compared to all other isolates.

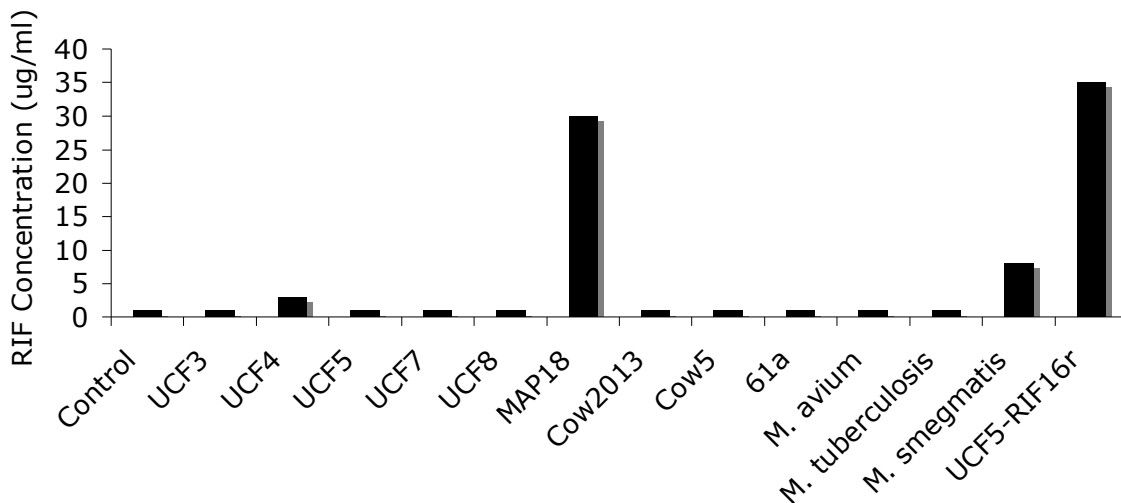


**Figure 7 Minimum Inhibitory Concentration (MIC) for each bacterial sample.**

The Y-axis represents the concentration of RIF expressed in ug/ml, while the X-axis represents all bacterial samples used for MIC testing. MAP18 and UCF5-RIF16r displayed similar MICs due to significant *rpoB* mutations. The MIC for MAP185 and UCF4 were slightly above that of the control, but not comparable to the resistant MAP strains. M. smegmatis displayed RIF resistance due to the bacterium's natural tendency for resistance against RIF.

### 3.5. UCF5-RIF16r

In order to determine the possibility of inducing in vitro RIF resistance in MAP, our wild-type MAP strain UCF5 was cultured in two-fold increases of RIF concentration initially beginning at a concentration of 1ug/ml. Over an extended time period, strain UCF5 was eventually increased to 16ug/ml, a concentration in which the strain had developed an adaptive resistance. After determining a high level of growth at this concentration, we then termed the newly resistant MAP strain UCF5-RIF16r. The adapted strain and was then maintained in cultures >16.0 ug/mL RIF thereafter.

Genomic DNA was extracted and followed by IS900-nested PCR and rpoB-based PCR analysis to investigate the possibility of a newly developed rpoB mutation. After strain UCF5-RIF16r was confirmed for the presence of IS900, and both regions of the rpoB gene were analyzed, we detected a single nucleotide rpoB mutation T1442C in the 81 bp variable region amplified by primers Knight1/Knight2, which caused a differentially expressed amino acid from Leu481 to Pro481 in the beta subunit of RNA polymerase (Fig 4, Table 3). The effect of this induced mutation on susceptibility to RIF was then investigated through susceptibility tests involving RIF as well as RFB. MAP strain UCF5-RIF16r was tested against RIF up to greater than 30 ug/mL and up to greater than 10 ug/mL for RFB. We determined that the MIC for UCF5-RIF16r against RIF and RFB was  $\geq 30$  ug/mL and  $\geq 10$  ug/mL, respectively (Fig 7, Table 3).

### 3.6. Blood Mixture

To show the potential for sequence analysis in the *rpoB* gene of MAP clinical isolates in correspondence with RIF and RFB resistance, we contaminated Human peripheral blood mononuclear cells (PBMNC) with  $1.0 \times 10^3$  CFU of MAP strain 18. Prokaryotic genomic DNA was then extracted from the blood mixture, followed by IS900-PCR and *rpoB*-based PCR analysis. As expected, our developed protocol detected MAP in the blood sample and successfully amplified both regions of the *rpoB* gene of MAP (data not shown). The nucleotide sequence was then analyzed for the possible prediction of susceptibility to RIF or RFB.

### 3.7. Taq Alignment

Specific amino acids are commonly known to alter upon resistance to RIF in *M. tuberculosis*, a close relative of MAP. Moreover, the *Thermus aquaticus* (Taq) beta subunit model has previously been provided and aligned with *M. tuberculosis*. In order to relate our current information with that previously shown, we aligned the variable region in MAP with *Thermus aquaticus* and *M. tuberculosis* for comparison purposes (Fig 8). Within the alignment (Fig 8) we provided a color coding scheme obtained from Campbell et al. 2001 corresponding to known amino acids positions and interaction data relevant to the RIF-Taq beta subunit complex. As displayed, colored dots indicate positions of amino acids relative to the bound RIF molecule. Amino acid alterations that have occurred in *M. tuberculosis* are also noted below their corresponding positions, and percentages are indicated for amino acid alterations that occur at high frequency upon RIF resistance in *M. tuberculosis*. Amino acid changes that occurred in MAP strain

18 and induced MAP strain UCF5-RIF16r within this region are indicated in bold at positions Thr456 and Leu481.

According to our alignment analysis of the MAP beta subunit relevant to the region shown in Figure 8, Arg388 in *Thermus aquaticus* overlaps that of Thr456 in MAP, and this amino is not considered to make significant interactions with bound RIF according to Campbell et. al 2001 (Fig 8). Moreover, Leu481 in MAP overlaps Leu413 in Taq, and this amino acid is considered to make significant Vanderwaals interactions with RIF in its bound state, possibly contributing to a more significant interaction with the drug. The significance of our alignment is that we may determine how the amino acid changes observed in MAP relate to commonly known residue changes that may occur in *M. tuberculosis*, and to predict positions and the significance of each amino acid within this region of the MAP beta subunit in relation to the available Taq model.



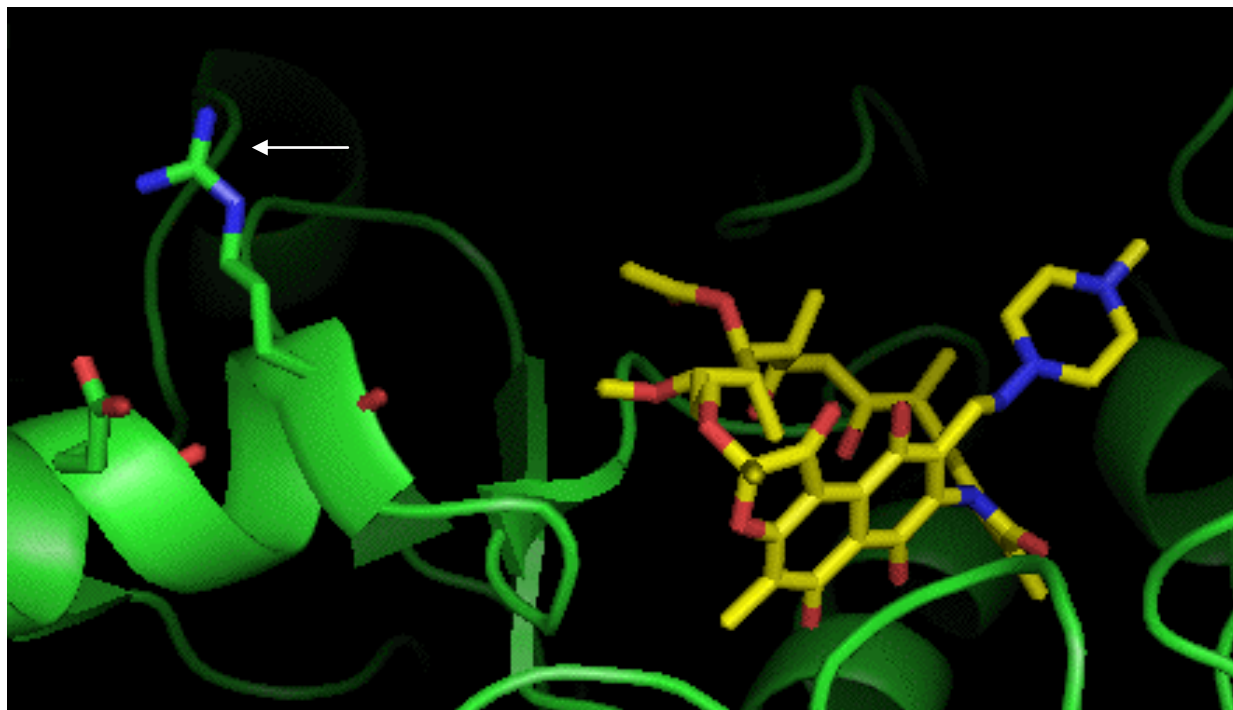
### 3.8. 3-D perspective

In order to obtain a photographic representation of the amino acid changes that occurred in MAP strains M18 and UCF5-RIF16r, we utilized the only available model available through PyMol Molecular-based Graphic program (DeLano 2005) for the display of RIF complexed with the beta subunit. The images shown are of the Taq model for the purpose of substituting for MAP. In order to view all PyMol images, we obtained protein database files from the RSBC PDB databank available through the [www.rcsb.org/pdb/home/home.do](http://www.rcsb.org/pdb/home/home.do) website. The specific pdb file that was utilized for visualization of Taq RIF complex model was 1YNN. Through this file, we were able to provide Figures 9, 10, 11, and 12.

#### 3.8.1 MAP strain 18 3-D model

The first displayed RIF complex model substitutes for MAP strain M18 (Fig 9). To describe, the Arg388 in *Thermus aquaticus* overlaps Thr456 in the beta subunit of MAP strain 18 (Fig 8). In *Thermus aquaticus*, this amino acid residue interacts with a nearby E384 within an alpha helix (Fig 9) which may contribute to the surrounding structure of the RIF pocket. As mentioned, we detected a Thr456 to Ile456 in MAP strain 18. We have shown this overlapping alteration from Arg388 to Ile388 in *Thermus aquaticus* for substitute for this change in MAP, and propose that this change may possibly reflect the observed increase in MIC due to a modification of the nearby structural atmosphere of the bound RIF (Fig 10). For example, if the surrounding lock structure for a key is altered, then the key will most likely not fit. More specifically, the Arg388 to Ile388 alteration may destabilize the alpha helix structure close to the RIF molecule, and

possibly affect the surrounding structure or pocket where RIF binds, resulting in a less stable RIF interaction.

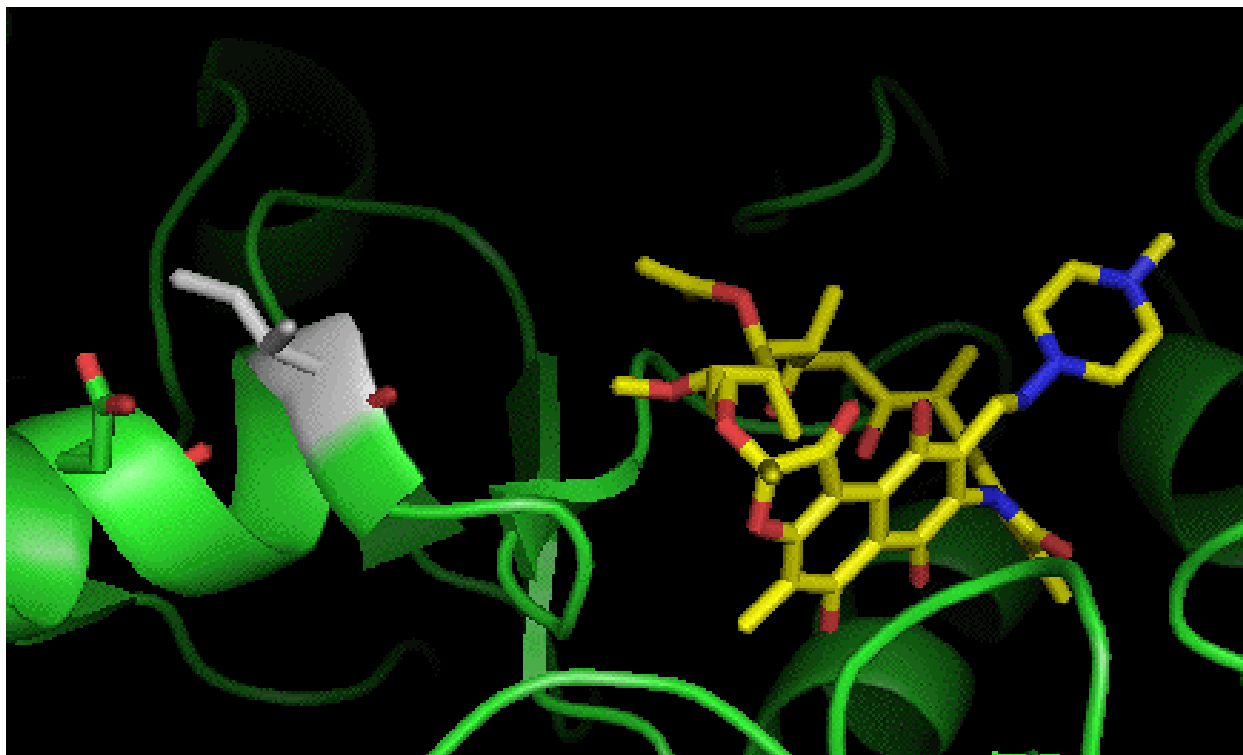


DeLano, W.L. MacPyMOL: A PyMOL-based Molecular Graphics Application for MacOS X (2005)

**Figure 9** *Thermus aquaticus* RIF complex model for MAP wildtype.

For *Thermus aquaticus*, R388 (Thr456 in MAP) is located within an alpha helix nearby the RIF antibiotic in its bound state. R388 is indicated by the white arrow. Surrounding beta subunit is shown as green and RIF antibiotic is shown as tan. Oxygen elements are shown as red and nitrogen elements are shown as blue.





DeLano, W.L. MacPyMOL: A PyMOL-based Molecular Graphics Application for MacOS X (2005)

**Figure 10** *Thermus aquaticus* RIF complex for resistant MAP strain 18.

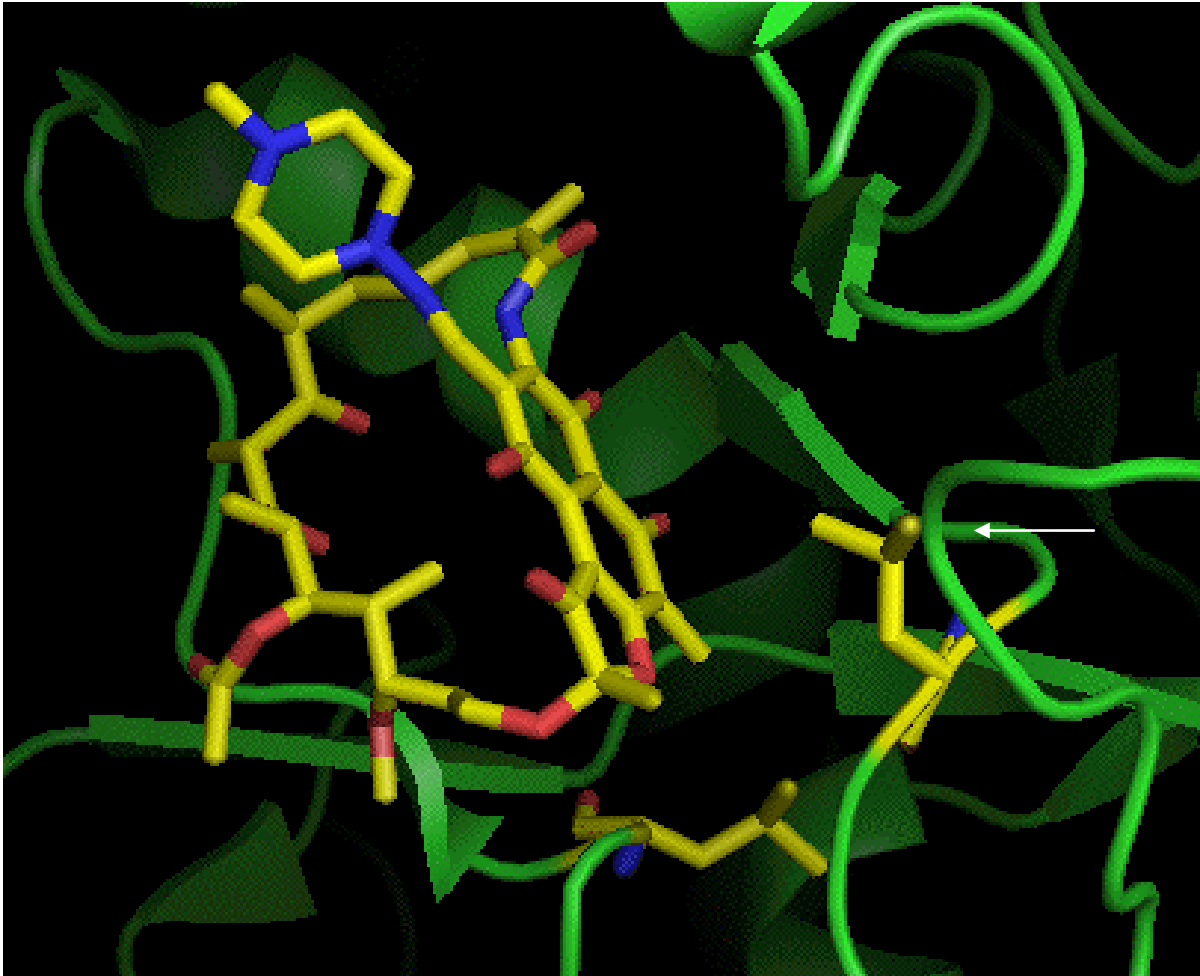
The specific alteration that is shown here is Arg388 to Ile388. This alteration represents that observed for MAP strain 18, Thr456 to Ile456. This alteration may possibly destabilize RIF interaction by altering a nearby alpha helical structure. The alteration is shown as gray, surrounding beta subunit is shown as green and RIF antibiotic is shown as tan. Oxygen elements are shown as red and nitrogen elements are shown as blue.

### 3.8.2 UCF5-RIF16r 3-D model

The second Taq RIF complex display substitutes for our wild-type MAP strain UCF5, as well as the induced MAP strain UCF5-RIF16r. To describe, Leu413 in *Thermus aquaticus*, which overlaps Leu481 in MAP (UCF5), interacts with Leu391 in close proximity to RIF in its bound state, contributes to Vanderwaal interactions with RIF, and may also contribute to the interactive stability between RIF and the beta subunit (Fig 11). As mentioned before, we have detected that a Leu481 to Pro481 alteration occurred in MAP strain UCF5-RIF16r upon resistance to RIF, and this alteration may also destabilize RIF interaction. An illustration of the Leu413 to Pro413 alteration in Taq is provided (Fig 12). To support our statement explaining the interaction between Leu481 and the RIF antibiotic, we have included a Taq RIF complex diagram provided by Campbell et. al. 2001 which shows Leu413 clearly interacting in close proximity to bound RIF (Fig 13).

### 3.8.3 Proposition

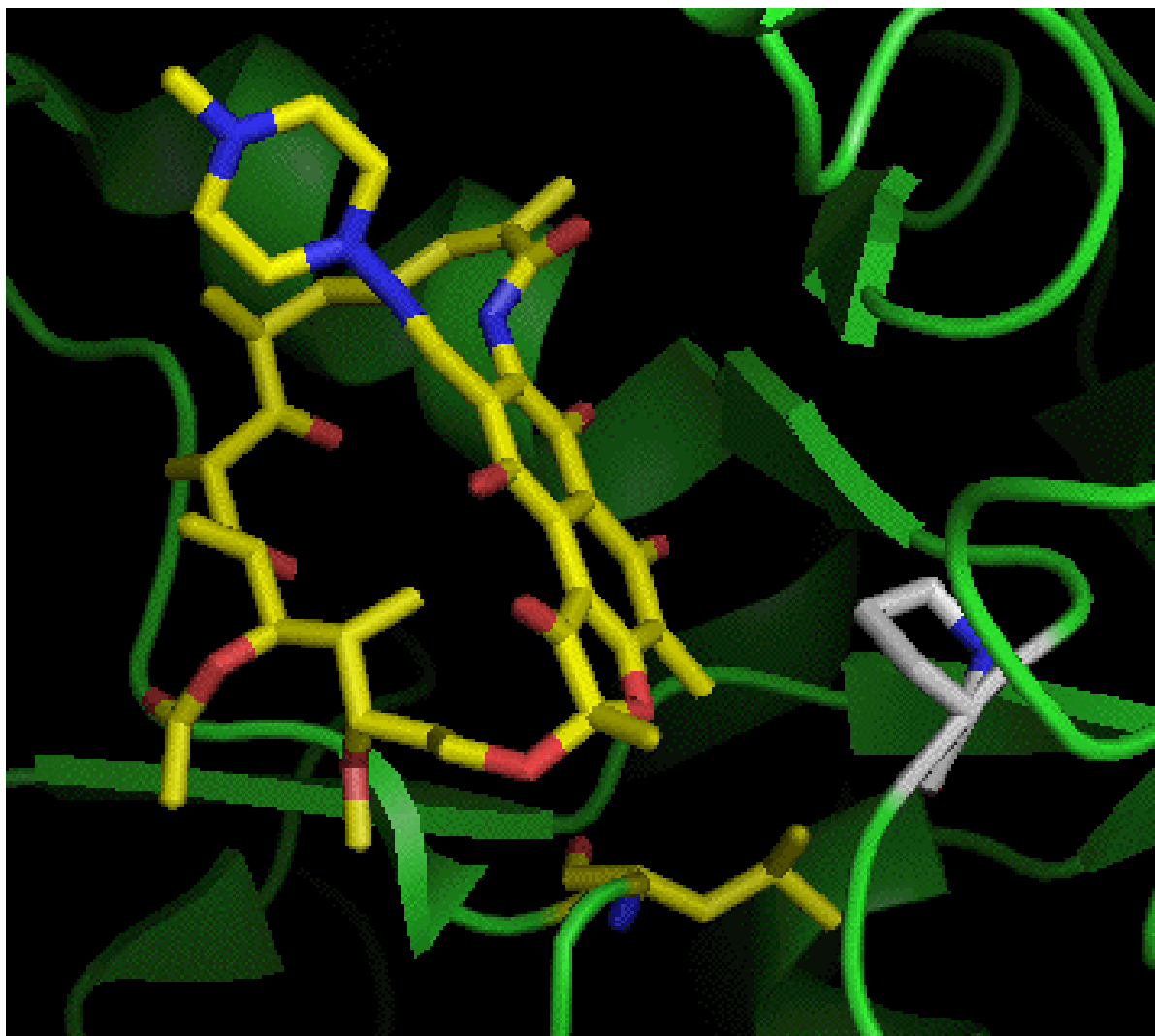
In both cases involving MAP strain M18 and UCF5-RIF16r, we propose that the amino acid alteration within this variable region causes a high level of resistance to RIF in MAP directly or indirectly. In addition, the changes observed do not affect the viability of for both strains. The *Thermus aquaticus* RNA polymerase RIF-complex provides an excellent model for illustrative purposes, and here we employ this available model to substitute for a visual representation of the overlapping amino acids observed in our resistant MAP strains.



DeLano, W.L. MacPyMOL: A PyMOL-based Molecular Graphics Application for MacOS X (2005)

**Figure 11** *Thermus aquaticus* RIF complex for wildtype MAP strain UCF5.

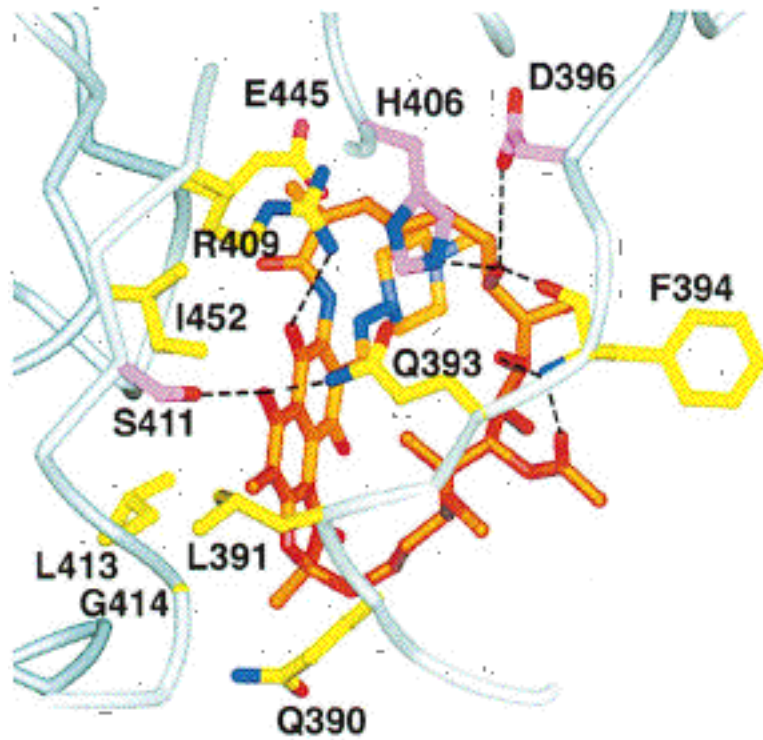
Both Leu391 and Leu413 make Vanderwaals interactions with RIF in its bound state. The white arrow indicates Leu413. Surrounding beta subunit is shown as green and RIF antibiotic is shown as tan. Oxygen elements are shown as red and nitrogen elements are shown as blue.



DeLano, W.L. MacPyMOL: A PyMOL-based Molecular Graphics Application for MacOS X (2005)

**Figure 12** *Thermus aquaticus* RIF complex for resistant MAP strain UCF-RIF16r.

The Leu413 to Pro413 alteration may contribute an interruption in Vanderwaals interactions between Leu413 and the RIF antibiotic, consequently destabilizing RIF interaction. The alteration is shown as gray, surrounding beta subunit is shown as green and RIF antibiotic is shown as tan. Oxygen elements are shown as red and nitrogen elements are shown as blue.



Campbell et al 2001

**Figure 13 Interactions with RIF and RNA polymerase.**

The Lue413 residue in T.a. overlaps that of Leu481 in MAP. This diagram clearly shows Leu413 in Taq interacting with bound RIF through Vanderwaals inteactions, as also previously stated by Campbell et at 2001.

### 3.9. Additional Sequencing

We attempted to sequence the entire 3.5 kb *rpoB* gene in order to determine the source of the variable increase in MIC for RIF against MAP strains UCF4, and to detect any other possible *rpoB* mutations leading to amino acid alterations in strains M18 and UCF5-RIF16r. Initially, we designed additional primers (Table 4) for PCR amplification of additional sequences outside of that amplified by primers UCF1/UCF2 and Knight1/Knight2. Our PCR results are shown in Figures 14-18, which represent the rest of the *rpoB* gene in each MAP strain mentioned. After successful PCR amplification of these regions, nucleotide sequencing was performed.

Blast analysis against the *rpoB* gene of MAP strain K-10 (wild-type) revealed a significant *rpoB* mutation further downstream of the region amplified by Knight1/Knight2 primers in MAP strain UCF4. Specifically, an A2284C mutation occurred within the region amplified by primers Ex1a/Ex2a. This mutation resulted in an Asn762 to His762 amino acid change, leading to a possible explanation for the observed higher MIC for RIF compared to our wildtype control strain 43544. Moreover, no other significant mutations were observed in MAP strains 18 and UCF5-RIF16r. The data clearly indicates that a single *rpoB* mutation may have considerable effects on RIF susceptibility in MAP, and that the region amplified by primers Knight1/Knight2 is highly significant for the analysis of *rpoB* mutations corresponding to RIF resistance.

**Table 4 Additional rpoB PCR primers.**

Primer Type and Name	Sequence (5' to 3")	Amplified Base Pairs (bp)*	Amplicon Length (bp)
rpoB			
Efox1	ttgccggccgaaccgacaca	1-721	721
Fox1r	tgtcgacgtcgaactccagc		
Fox1f	cgggttcatgggtgacttc	521-1509	989
DBR	gtagtgggacgggtgcacgtc		
Ex1a	aaggtggtcgacggcgtggt	1621-2340	720
Ex2a	gatctcgtgctcctcgatgt		
Ex3	acgaggacgcatcatcct	2261-2980	720
Ex4	tcgacacgatctggttcggc		
Ex5	gaacatcgacggcaatcccg	2901-3597	697
Hrox1	tccgtcgaggacctggcttaa		

\*Numbers represent nucleotide positions within the rpoB gene of MAP. and  $\geq 9.0$  ug/mL,

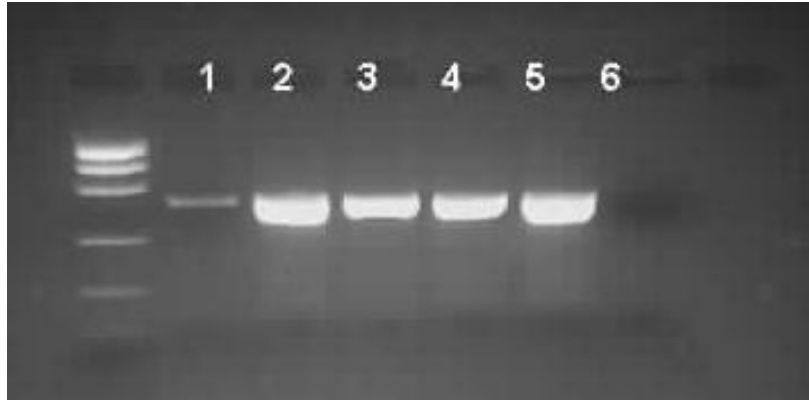


**Figure 14** *rpoB* PCR results using Efox1/Fox1r primers.

Each lane corresponds to the following MAP strains: 1, 43544 (positive control); 2, UCF4; 3, M18; 4, UCF5-RIF16r; 5, M185; 6, negative control.

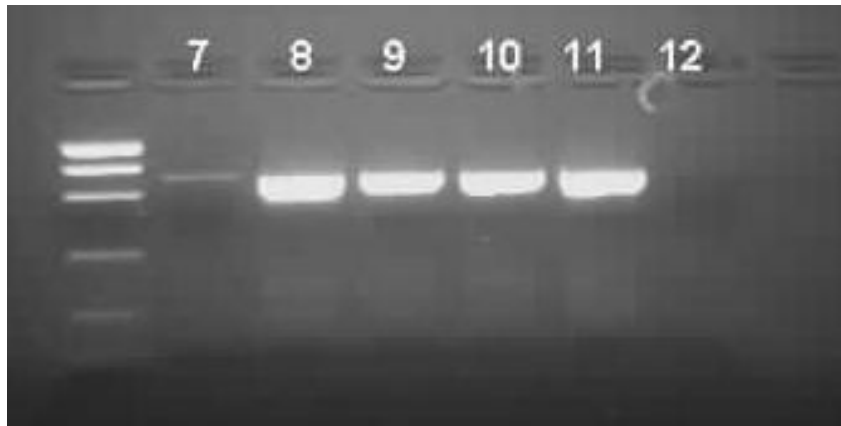


**Figure 15** *rpoB* PCR results using Fox1/DBR primers.

Each lane corresponds to the following MAP strains: 7, 43544 (positive control); 8, UCF4; 9, M18; 10, UCF5-RIF16r; 11, M185; 12, negative control.



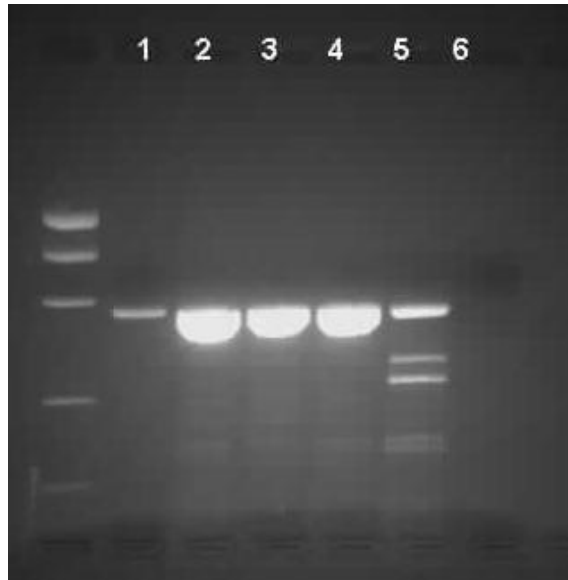


**Figure 16** rpoB PCR results using Ex1a/Ex2a primers.

Each lane corresponds to the following MAP strains: 1, 43544 (positive control); 2, UCF4; 3, M18; 4, UCF5-RIF16r; 5, M185; 6, negative control.

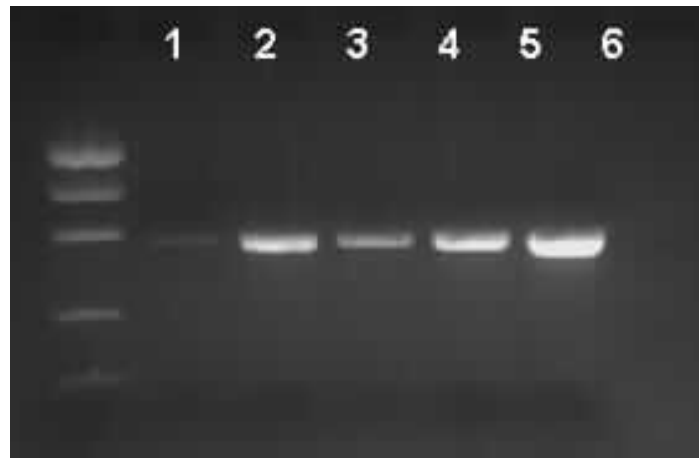


**Figure 17** rpoB PCR results using Ex3/Ex4 primers.

Each lane corresponds to the following MAP strains: 1, 43544 (positive control); 2, UCF4; 3, M18; 4, UCF5-RIF16r; 5, M185; 6, negative control.

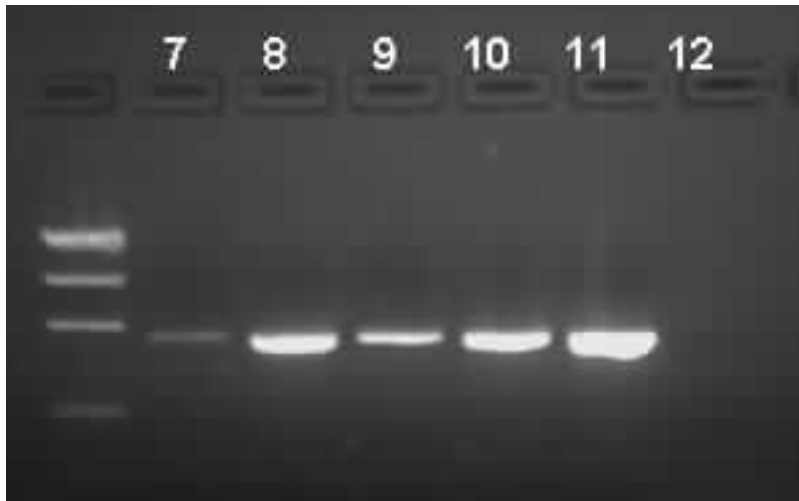
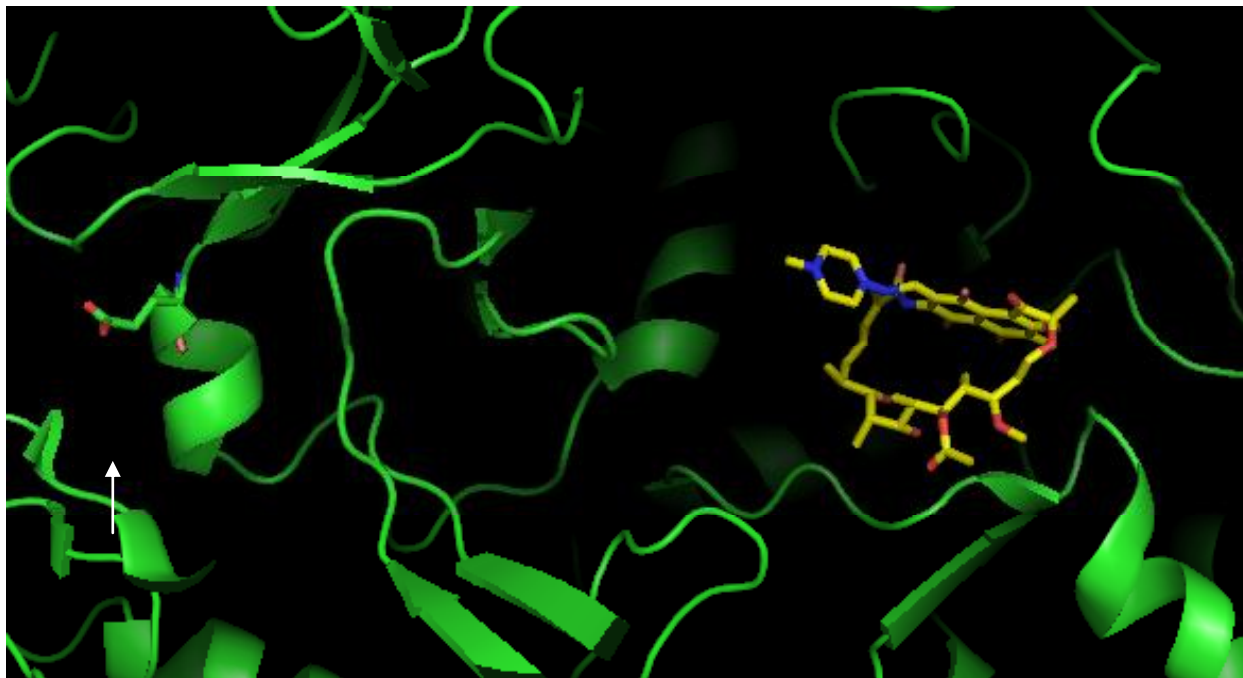


**Figure 18** *rpoB* PCR results using Ex5/Hrox1 primers.

Each lane corresponds to the following MAP strains: 7, 43544 (positive control); 8, UCF4; 9, M18; 10, UCF5-RIF16r; 11, M185; 12, negative control.

### 3.10. UCF4 3-D model

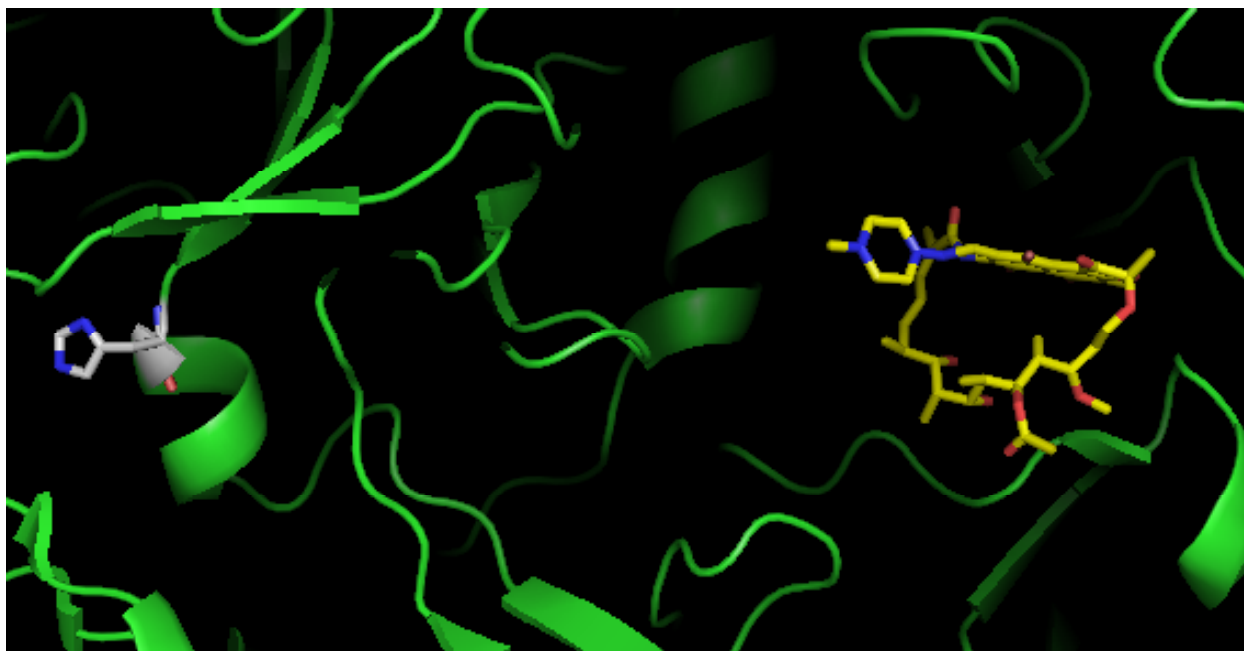
After obtaining the entire rpoB sequence for MAP strain UCF4, which revealed a A2284C mutation causing a Asn762 to His762 amino acid change, we provided a third Taq RIF complex display to illustrate the observed alteration in the beta subunit. To explain, Glu692 in Taq overlaps Asn762 in MAP, and this amino acid lies within an alpha helical structure somewhat distant from RIF in its bound state (Fig 19). The Glu692 to His692 change shown in Figure 20 represents the Asn762 to His762 alteration in MAP strain UCF4. Reverting back to our lock and key example, we propose that the surrounding RIF pocket is again modified, however our RIF susceptibility tests for strain UCF4 indicate that the modification within the beta subunit was not as detrimental as compared to MAP strains M18 and UCF5-RIF16r.



DeLano, W.L. MacPyMOL: A PyMOL-based Molecular Graphics Application for MacOS X (2005)

**Figure 19** *Thermus aquaticus* RIF complex for wild-type MAP.

The Glu692 is indicated by the white arrow, and contributes to the alpha helical structure shown. Glu692 in this Taq model substitutes for Asn762 in wild-type MAP. Surrounding beta subunit is shown as green and RIF antibiotic is shown as tan. Oxygen elements are shown as red and nitrogen elements are shown as blue.



DeLano, W.L. MacPyMOL: A PyMOL-based Molecular Graphics Application for MacOS X (2005)

**Figure 20** *Thermus aquaticus* RIF complex for MAP strain UCF4.

The specific alteration that is shown here is Glu692 to His692 in Taq, which substitutes for the Asn762 to His762 change seen in MAP strain UCF4. This change may possibly explain the variable increase in MIC against RIF for strain UCF4. The alteration is shown as gray, surrounding beta subunit is shown as green and RIF antibiotic is shown as tan. Oxygen elements are shown as red and nitrogen elements are shown as blue.

### 3.11. Entire rpoB Sequence

After collective analysis of our rpoB PCR and sequencing results, we were able to display the entire rpoB gene sequence for MAP strains K-10, (wild-type control sequence), M18, UCF5-RIF16r, and UCF4,. The ability to display this information was a direct consequence of our successful PCR and sequencing reactions involving the primers described in Table 2 and Table 4. Figures 21, 22, 23, and 24, allow a clear observation of the significant nucleotide positions C1367, T1442 and A2284 relative to the rest of the rpoB gene. The 81 bp region is bolded for all complete gene sequence figures 21,22,23, and 24 and the corresponding nucleotide mutations are indicated as blue bold for silent, and red bold for amino acid-changing. Notice that the rpoB mutation for MAP strain UCF4 is outside of the 81 bp variable region, and as mentioned before, this mutation led to a less significant change in the MIC against RIF. This indicates that the significant region for detection of RIF resistance in MAP is located within the 81 bp bolded region shown.

1 ttgccggccg aaccgacaca attcgcggcg aacgcagccg gtggtcccgg ccttcgtgag  
61 tcgacagagg tgctggaagg atgcatcttg gcagattcc gccagagcaa gacggatcgc  
121 ccacaaagt cctcaaacgg atcaagtcc ttgaacggct ccgtgcccgg agcggccaac  
181 cgagtttct tcgccaagct gcggaaccg ctcgaggttc ccggcctgct ggacgtgag  
241 atcgactct tcgagtggt gatcggcgcg ccgcggtggc gtgaggccgc gatcggccc  
301 ggcgacgcg agccaaggg cgggtggaa gaggtgctc acgagctgc gccgatcga  
361 gacttctcg gctcgtatg gctgtcttc tccgacccc gcttcgacga ggtcaaggc  
421 ccggtcgacg agtgcaaaga caaggacatg acgtacgcg ccccgtgtt cgtcacggc  
481 gagttcatca acaacaacac cggcgagatc aagagccaga cgggttcat ggtgacttc  
541 ccgatgatga ccgagaaggg caccttcac atcaacggga ccgagcgcgt ggtggtcagc  
601 cagctggtcc gctgcgggg cgtgtactc gacgagacca tcgacaagtc caccgagaag  
661 acgctgcaca gctcaagg gatccccagc cgcggcgct ggctggagtt cgacgtcag  
721 aagcgcgaca ccgtcggct gcgcatcgc cgaagcgc gccagccgt caccgtgctg  
781 ctaaggcgc tgggtggac caacgagcag atcaccgagc ggttcggtt ctcgagatc  
841 atgatgcga cgctggagaa ggacaacacc gccggcaccg acgaggcgt gctggacatc  
901 taccgcaag tcgcccggg cgagccgcg accaaggagt ccgcgacag cctgctggag  
961 aacctgtt tcaaggagaa gcgctacgac ttggcccggg tgggccccta caaggtaac  
1021 aagaagctc ccctgcacgc cgtgagccg atcaccagct cgacgtgac cgaggaagac  
1081 gtctgcgca ccatcgagta cctggtcgc ctgacgagg gtcagcccac gatgaccgt  
1141 ccggcgccga tcgagtgcc ggtggagacc gacgacatc accactcgg caaccgccc  
1201 ctgcgcaccg tcggtgagct gatccagaac cagatccgg tcggcatgct ccggatggag  
1261 cgcgtcgtcc gcgagcggat gaccacccag gacgtcagc ccatcacgcc gcagaccctg  
1321 atcaacatcc gtcccgtct ggcggcgtc aaggagtct **tcggcaccag ccagttgtcc**  
**1381 cagttcatgg accagaacaa cccgctgctg gggctcacc acaagcggc cctgtcggcg**  
**1441 ctgggcccgg gtggtctgc ccgggagcgg gccgggctgg aggtccgca cgtcacccg**  
1501 tccactacg gccgatgtg ccgatcag acccggagg gtccaacat cgtctgatc  
1561 ggctcgtgt cgtgtacgc gcgggtcaac ccgtcgggt tcatcgagac gccgtaccg  
1621 aagtggtgc acggtgtgt caccgacgag atccactacc tgaccgccga cgaggaggac  
1681 cgccacgtg tggcgcagg caactcggc atcgacgaca agggccggt cgccgaggc  
1741 cgggtgctg tccgcccaa ggcggcgag gtcgagtac tgccctcgt cgaggtggac  
1801 tacatggacg tgaaccgc ccagatggt tcggtggca ccgcatgat cccgttctc  
1861 gagcacgacg acgccaaccg tgccctgat gccgccaaca tcagcgcga gccggttccg  
1921 ctggtgcga gcgagggccc gctggtggc accggcatgg agctcgtgc cgcgatcga  
1981 gccggcagc tcgtcgtcgc cgagaagtcc ggggtgatc aggaggttc cgccgactac  
2041 atcaccgtg tggccgacga cggcaccgg cacacctacc ggatgcgca gttcagcgg  
2101 tcaaccacg gcacctgct caaccagac ccgatcgtc acgcccgca ccgggtcag  
2161 gccggccagg tcatcgcca cgttccgtc accgagaac gcgagatgg cctgggcaag  
2221 aacctgctg tgggatcat gccgtggag ggccacaact acgaggacgc gatcatctc  
2281 tcaaccggc tgggtgagga ggacgtgtg acgtccatc acatcgagga gcagagatc  
2341 gacggccgc acaccaagt gggcgccgag gagatcacc gggacatccc gaacgtctc  
2401 gacgaggtg tggccgacct ggacgagcgc ggcacgtgc gcatcggcg cgaggtccg  
2461 gacggcgaca tcctggtcgg caaggtcacc ccgaagggg agaccgagct gacggcgag  
2521 gagcgctgc tcgcgccat ctcggcgag aaggcccgc aggtccgca cactcgtc  
2581 aagtgccg acggcgagtc cggcaaggc atcggcatc cgggtgttc ccgagaggc  
2641 gacgacgagc tgcccggcgg ggtcaacgag ctggtccgc tctacgtgg ccagaagcg  
2701 aagatctcc aggtgacaa gctcggcgc cggcacggca acaagggcgt catcggcaag  
2761 atcctgccg agggagacat gccgttcta ccggacggca cggcgtgga catcatctg  
2821 aacaccacg gttgcccgc acggatgaac atcggccaga tctggagac ccactggg  
2881 tgggtggca agtccggct gaacatcgc ggcaatccc agtggcggt caactgccc  
2941 gaggagctg ggcacgcaca gccgaaccg atcgttgcg caccggtgt cgacggcgc  
3001 aaggaagagg agctggccc catgctgctg tcacgctgc ccaaccgca cggcgaggtc  
3061 atggtgacg gcgacggca ggcggtgct ttcgacggc ggtccggga gccgtccc  
3121 taccggta ccgtcgcta catgtacat atgaagctg accacctgt ggacgacaag  
3181 atccacgcc gctccaccg ccgtactc atgatcacc agcagccgt gggcgtaag  
3241 gcgagttc gtggcagc ctcggtgag atggagtgt gggccatga ggcctacgg  
3301 gcggcgta ccgtgcagga gctgtgacc atcaagtcg acgacacgt cggccgggtc

3361 aaggtgtacg aggcgatcgt caagggcgag aacatcccgg agccgggtat ccccgagtcc  
3421 ttcaaggtgt tgctcaagga gctgcagtcg ctgtgcctca acgtcgaggt gctctcctcc  
3481 gacggcgcgg ccatcgagct gcgcgaaggc gaggacgagg acctggagcg ggccgcggcg  
3541 aacctgggaa tcaactgtc ccgcaacgaa tccgcgtccg tcgaggacct ggcttaa

**Figure 21 Entire rpoB gene sequence for MAP strain K-10, wild-type control sequence (Li et al 2005).**

The 81 bp variable region is bolded and located between nucleotides 1363 and 1443.



1 ttgccggccg aaccgacaca attcgcggcg aacgcagccg gtggtcccgg ccttcgtgag  
61 tcgacgagg tgctggaagg atgcatctg gcagattcc gccagagcaa gacggatcgc  
121 ccacaaagt cctcaaacgg atcaagtcc ttgaacggct ccgtgcccgg agcggccaac  
181 cgagtttct tcgcaagct gcgcaaccg ctcgaggttc ccggcctgct ggacgtgacg  
241 atcgactct tcgagtgggt gatcgggcgc cgcgggtggc gtgaggccgc gatcggccc  
301 ggcgacgcg agccaaggg cgggtggaa gaggtgctc acgagctgc gccgatcgag  
361 gacttctcg gctcgatgc gctgtcttc tccgacccc gcttcgacga ggtcaaggc  
421 ccggtcgacg agtcaaaga caaggacatg acgtacgcg ccccgtgtt cgtcacggc  
481 gagttcatca acaacaacac cggcgagatc aagagccaga cgggttcat ggtgacttc  
541 ccgatgatga ccgagaaggg caccttcac atcaacggga ccgagcgcgt ggtggtcagc  
601 cagctggtcc gctgcgggg cgtgtactc gacgagacca tcgacaagtc caccgagaag  
661 acgctgcaca gcgtcaagg gatccccagc cgcggcgct ggttgaggt cgacgtcagc  
721 aagcgcgaca ccgtcggct gcgcatcgc cgaagcgc gccagccgt caccgtgctg  
781 ctaaggcgc tgggtggac caacgagcag atcaccgagc ggttcggtt ctcgagatc  
841 atgatgcga cgctggagaa ggacaacacc gccggcaccg acgaggcgt gctggacatc  
901 taccgaagc tgcggccgg cgagccgccc accaaggagt ccgcgacagc cctgctggag  
961 aacctgtt tcaaggaaa gcgctacgac ctggcccggg tgggccccta caagtaaac  
1021 aagaagctc ccctgcacgc cgtgagccg atcaccagct cgacgtgac cgaggaagac  
1081 gtctgcga ccatcgagta cctggtcgc ctgcacgag gtcagcccac gatgaccgt  
1141 ccggcgcca tcgagtgcc ggtggagacc gacgacatc accactcgg caaccgccc  
1201 ctgcgcaccg tcggtgagct gatccagaac cagatccgg tcggcatgic ccggatggag  
1261 cgcgtctcc gcgagcggat gaccaccag gacgtcagc ccatcacgc gcagaccctg  
1321 atcaacatcc gtcccgtct ggcggcgc atcaggattt tggcactag ccagtgtcc  
**1381 cagttcatgg accagaaca cccgctgctg gggctaccc acaagcggc cctgctggcg**  
**1441 ctgggcccgg gtggtctgc ccgggagcgg gccgggctgg aggtccgca cgtgcaccg**  
1501 tccactacg gccgatgtg cccgatcag acccggagg gtccaacat cgtctgatc  
1561 ggtcgtctg cgggtacgc gcggtaac ccgtccggg tcatcgagc gccgtaccg  
1621 aaggtggtc acgctggtt caccgacgag atccactacc tgaccgcca cgaggaggac  
1681 cgccaagtg tggcgaggc caactcggc atcgacgaca agggccggt cgcgaggcc  
1741 cgggtgctg tccgcccaa ggcggcgag gtcgagtac tgccctcgc cgaggggac  
1801 tacatggacg tgtaccgac ccagatggtg tcggtgcca ccgcatgat cccgttctc  
1861 gagcacgacg acgccaaccg tgccctgat ggcgccaaca tcagcgcca ggcggtccg  
1921 ctggtgcga gcgaggcgc gctggtggc accggcatg agctcgtgc cgcgatcgc  
1981 gccggcagc tcgtcgtcgc cgagaagtcc ggggtgatc aggaggtct cgcgactac  
2041 atcaccgtg tggccgacg cggcaccgg cacacctacc ggatgcgca gttcagcgg  
2101 tcaaccacg gcacctgac caaccagagc ccgatcgtc acgcccgca ccgggtcag  
2161 gccggcagg tcatcgcca cgtccctgc accgagaacg gcgagatgg gctgggcaag  
2221 aacctgctg tgggatcat gccgtggag ggccacaact acgaggacgc gatcatctc  
2281 tcaaccggc tgggtgagga ggacgtgtg acgtccatc acatcgagga gcacgagatc  
2341 gacggcgcg acaccaagt gggcggcag gagatcacc gggacatcc gaactctc  
2401 gacgaggtg tggccgacct ggacgagcgc ggatcgtgc gcatcggcgc cgaggtccg  
2461 gacggcgaca tctggtcgg caaggtcacc ccgaagggg agaccgagct gacggcgag  
2521 gagcggctg tcgcgccat cttcggcag aaggcccgc aggtccgca cacctcgtg  
2581 aaggtgccg acgcgagtc cggcaagtc atcgatcc ggtgttctc ccgagaggc  
2641 gacgacgagc tgcccggcg ggtcaacgag ctggtccgc tctacgtggc ccagaagcgc  
2701 aagatctcc acggtgaca gctcggcgc cggcagggc acaagggcgt catcggcaag  
2761 atcctgccg aggaggacat gccgttcta ccggacggc cgcgggtgga catcatcctg  
2821 aacaccacg gtgtccgcg acggtgaac atcggccaga tctggagac ccactgggg  
2881 tgggtggca agtccgctg gaacatcgc ggcaatccc agtggcggg caactgccc  
2941 gaggagtgc ggcacgcaca gccgaaccag atcgtgtcga caccggtgt cgacggcgc  
3001 aaggaagag agctggccc catgctgtc tgcacgtgc ccaaccgca cggcgagtc  
3061 atggtgacg gcgacggca ggcggtgct tgcacggcc ggtccggga cccgtcccg  
3121 taccgggta ccgtcgcta catgtacatc atgaagctgc accactggt ggacgacaag  
3181 atccacgccc gctccaccg cccgtactc atgatcacc agcagccgt gggcgtaag  
3241 gcgagttcgt gggccagc cttcgtgag atggagtgt gggccatgca ggcctacgg

3301 gcggcgtaca cgctgcagga gctgtgacc atcaagtccg acgacacggt cggccgggtc  
3361 aaggtgtacg aggcgatcgt caagggcgag aacatcccgg agccgggtat ccccgagtcc  
3421 ttcaagggtg tgctcaagga gctgcagtcg ctgtgcctca acgtcgaggt gctctcctcc  
3481 gacggcgcgg ccatcgagct gcgcgaaggc gaggacgagg acctggagcg ggccgcggcg  
3541 aacctgggaa tcaactgtc ccgcaacgaa tccgcgtccg tcgaggacct ggcttaa

**Figure 22 Entire rpoB gene sequence for MAP strain M18.**

**The C1367T and T1375C mutations are indicated bold with their corresponding colors and increased font. Red bold circled positions correspond to mutations that caused an amino acid alteration, and blue bold correspond to silent mutations.**

1 ttgccggccg aaccgacaca attcgcggcg aacgcagccg gtggtcccgg ccttcgtgag  
61 tcgcacgagg tgctggaagg atgcatcttg gcagatttcc gccagagcaa gacggatcgc  
121 ccacaaagt cctcaaacgg atcaagtcc ttgaacggct ccgtgcccgg agcggccaac  
181 cgagtttct tcgcaagct gcgcgaaccg ctcgaggttc ccggcctgct ggacgtgca  
241 atcgactct tcgagtgggt gatcggcgcg ccgcggtggc gtgaggccgc gatcggccc  
301 ggcgacgcgg agccaaggg cgggttgaa gaggtgctcg acgagctgc gccgatcgag  
361 gacttctcgg gctcgatgc gctgtcttc tccgacccc gcttcgacga ggtcaaggcg  
421 ccggtcgacg agtgcaaaga caaggacatg acgtacgcg ccccgtgtt cgtcacggcc  
481 gagttcatca acaacaacac cggcgagatc aagagccaga cgggttcat ggtgacttc  
541 ccgatgatga ccgagaaggg caccttcatc atcaacggga ccgagcgcgt ggtggtcagc  
601 cagctggtcc gctgcgggg cgtgtacttc gacgagacca tcgacaagtc caccgagaag  
661 acgctgcaca gcgtcaagg gatccccagc cgcggcgctt ggctggagtt cgacgtcagc  
721 aagcgcgaca ccgtcggcgt gcgcatcgac cgcaagcgc gccagccggt caccgtgctg  
781 ctaaggcgc tgggtggac caacgagcag atcaccgagc ggttcggctt ctccgagatc  
841 atgatgcga cgctggagaa ggacaacacc gccggcaccg acgaggcgt gctggacatc  
901 taccgaagc tgcggccgg cgagccgccc accaaggagt ccgcgacagc cctgctggag  
961 aacctgtt tcaaggaa gcgctacgac ctggcccggg tgggccccta caaggtcaac  
1021 aagaagctg ccctgcacgc cgtgagccg atcaccagct cgacgtgac cgaggaagac  
1081 gtctgcgca ccatcgagta cctggtcgc ctgcacgagg gtcagcccac gatgaccgtc  
1141 ccggcgccga tcgagtgcc ggtggagacc gacgacatcg accactcgg caaccgccc  
1201 ctgcgcaccg tcggtgagct gatccagaac cagatccggg tcggcatgct ccggatggag  
1261 cgcgtcgtcc gcgagcggat gaccacccag gacgtcgagg ccatcacgcc gcagaccctg  
1321 atcaacatcc gtcccgtct ggcggcgatc aaggagtct **tcggcaccag ccagttgtcc**  
**1381 cagttcatgg accagaacaa cccgctgctg gggctcacc acaagcgcg cctgtcggcg**  
**1441 cC**gggcccgg gtggtctgct ccgggagcgg gccgggctgg aggtccgca cgtgcaccg  
1501 tcccactacg ccggatgtg cccgatcgag accccgagg gtccaacat cgtctgatc  
1561 ggtcgtctgt cgggtacgc gcgggtcaac ccgttcgggt tcatcgagac gccgtaccg  
1621 aaggtggtc acgctgtgt caccgacgag atccactacc tgaccgccga cgaggaggac  
1681 cgccaagtg tggcgaggc caactcggc atcgacgaca agggccggtt cgccgaggcc  
1741 cgggtgctg tccgcccaa ggcggcgag gtcgagtacg tgccctcgtc cgaggtggac  
1801 tacatggacg tgtaccgcg ccagatggtg tcggtggcca ccgcatgat cccgttctc  
1861 gagcacgacg acgccaaccg tgccctgatg ggcgccaaca tcagcgcga ggcggttccg  
1921 ctggtgcga gcgagggccc gctggtggc accggcatgg agctgcgtgc cgcgatcgac  
1981 gccggcgacg tcgtcgtcgc cgagaagtcc ggggtgatc aggaggtctc cgccgactac  
2041 atcaccgtga tggccgacga cggcaccgg cacacctacc ggatgcgca gttcagcgg  
2101 tcaaccacg gcacctgac caaccagagc ccgatcgtc acgcccgca ccgggtcgag  
2161 gccggccagg tcatcgcca cgtccctgc accgagaacg gcgagatgg gctgggcaag  
2221 aacctgctg tgggatcat gccgtgggag ggccacaact acgaggacgc gatcatctc  
2281 tcaaccggc tgggtgagga ggacgtgtg acgtccatc acatcgagga gcacgagatc  
2341 gacggccgc acaccaagct gggcgccgag gagatcacc gggacatccc gaactctc  
2401 gacgaggtg tggccgacct ggacgagcgc ggatcgtgc gcatcggcgc cgaggtccg  
2461 gacggcgaca tctggtcgg caaggacc ccgaagggg agaccgagct gacggcgag  
2521 gagcggctg tcgcgccat cttcggcgag aaggcccgc aggtccgca cacctcgtg  
2581 aaggtgccg acggcgagtc cggcaaggtc atcggatcc ggtgttctc ccgagaggac  
2641 gacgacgagc tgcccggcg ggtcaacgag ctggtccgc tctacgtggc ccagaagcgc  
2701 aagatctcc acggtgaca gctgcggc cggcacggca acaagggcgt catcggcaag  
2761 atcctgccg aggaggacat gccgttcta ccggacggca cggcggtgga catcatctg  
2821 aacaccacg gtgtcccg acggatgaac atcggccaga tctggagac ccactggg  
2881 tgggtggca agtccgctg gaacatcgac ggcaatccc agtggcggt caactgccc  
2941 gaggagctg ggcacgcaca gccgaaccag atcgtgtcga caccggtgtt cgacggcgc  
3001 aaggaagag agtggcccg catgctgtc tgcacgtgc ccaaccgca cggcgaggtc  
3061 atggtgacg gcgacggca ggcggtgct ttcgacggc ggtccgggga cccgttccc  
3121 taccgggta ccgtcgcta catgtacatc atgaagctgc accactggt ggacgacaag  
3181 atccacgccc gctccaccg cccgtactc atgatcacc agcagccgct gggcgtaag  
3241 gcgagttcgt gggccacg cttcggtgag atggagtgt gggccatgca ggcctacgg

3301 gcggcgtaga cgctgcagga gctgtgacc atcaagtccg acgacacggt cggccgggtc  
3361 aaggtgtacg aggcgatcgt caagggcgag aacatcccgg agccgggtat ccccgagtcc  
3421 ttcaagggtg tgctcaagga gctgcagtcg ctgtgcctca acgtcgaggt gctctcctcc  
3481 gacggcgagg ccatcgagct ggcggaaggc gaggacgagg acctggagcg ggccgcggcg  
3541 aacctgggaa tcaactgtc ccgcaacgaa tccgcgtccg tcgaggacct ggcttaa

**Figure 23 Entire rpoB sequence for induced MAP strain UCF5-RIF16r.**

The T1442C mutation caused an amino acid change in this strain. Red bold circled positions correspond to mutations that caused an amino acid alteration, and blue bold correspond to silent mutations.

1 ttgccggccg aaccgacaca attcgcggcg aacgcagccg gtggtcccgg ccttcgtgag  
61 tcgacgagg tgctggaagg atgcatctg gcagattcc gccagagcaa gacggatcgc  
121 ccacaaagt cctcaaacgg atcaagtcc ttgaacggct ccgtgcccgg agcggccaac  
181 cgagtttct tcgccaagt gcgcaaccg ctcgaggttc ccggcctgct ggacgtgag  
241 atcgactct tcgagtggt gatcggcgcg ccgcggtggc gtgaggccgc gatcggccc  
301 ggcgacgcg agccaaggg cgggtggaa gaggtgctc acgagctgc gccgatcga  
361 gacttctcg gctcgatgc gctgtcttc tccgacccc gcttcgacga ggtcaaggc  
421 ccggtcgacg agtgcaaaga caaggacatg acgtacgcg ccccgtgtt cgtcacggc  
481 gagttcatca acaacaacac cggcgagatc aagagccaga cgggttcat ggtgacttc  
541 ccgatgatga ccgagaaggg caccttcac atcaacggga ccgagcgcgt ggtggtcagc  
601 cagctggtcc gctgcgggg cgtgtactc gacgagacca tcgacaagtc caccgagaag  
661 acgctgcaca gcgtcaagg gatccccagc cgcggcgct ggctggagtt cgacgtcag  
721 aagcgcgaca ccgtcggct gcgcatcgc cgaagcgc gccagccgt caccgtgctg  
781 ctaaggcgc tgggtggac caacgagcag atcaccgagc ggttcggct ctcgagatc  
841 atgatgcga cgctggagaa ggacaacacc gccggcaccg acgaggcgt gctggacatc  
901 taccgaagc tgcggccgg cgagccgccc accaaggagt ccgcgacagc cctgctggag  
961 aacctgtct tcaaggaaa gcgctacgac ctggcccggg tgggcccgta caaggtaac  
1021 aagaagctcg ccctgcacgc cgtgagccg atcaccagct cgacgtcag cgaggaagac  
1081 gtcgtcgcca ccatcagta cctggtcgc ctgcacgagg gtcagcccac gatgaccgt  
1141 ccggcgccga tcgagtgcc ggtggagacc gacgacatc accacttcg caaccgccc  
1201 ctgcgcaccg tcggtgagct gatccagaac cagatccgg tcggcatgct ccggatggag  
1261 cgcgtcgtcc gcgagcggat gaccacccag gacgtcaggg ccatcacgcc gcagaccctg  
1321 atcaacatcc gtcccgtct ggcggcgtc aaggagtct **tcggcaccag ccagttgtcc**  
**1381 cagttcatgg accagaacaa cccgctgctg gggctcacc acaagcgcg cctgtcggcg**  
**1441 ctgggcccgg gtggtctgc ccgggagcgg gccgggctgg aggtccgca cgtcacccc**  
1501 tccactacg gccgatgtg ccgatcag acccggagg gtccaacat cgtctgatc  
1561 ggctcgtgt cgtgtacgc gcgggtcaac ccgtcgggt tcatcagac gccgtaccg  
1621 aaggtgctg acggcgtgt caccgacgag atccactacc tgaccgccga cgaggaggc  
1681 cgccacgtg tggcgcagg caactcggc atcagcaca agggccggt cggcaggcc  
1741 cgggtgctg tccgcccaa ggcggcgag gtcagtagc tgccctcgt cgaggtggac  
1801 tacatggacg tgaaccgcg ccagatggtg tcggtggcca ccgcatgat cccgttctc  
1861 gagcacgacg acgccaaccg tgccctgat ggcgccaaca tcagcgcga gccggttccg  
1921 ctggtgcga gcgagggccc gctggtggc accggcatgg agctgcgtgc cgcgatcga  
1981 gccggcagc tcgtcgtgc cgagaagtcc ggggtgatc aggaggtct cggcactac  
2041 atcaccgtg tggccgacga cggcaccgg cacacctacc ggatgcgca gttcagcgg  
2101 tcaaccacg gcacctgct caaccagag ccgatcgtc acgcccgga ccgggtcag  
2161 gccggccagg tcatcggca cgttccgtc accgagaac gcgagatgg gctgggcaag  
2221 ~~aacctgctg~~ tggcgtcat gccgtggag ggccaact acgaggacgc gatcatctc  
2281 **tcc**<sup>C</sup>accgctg ggttgagga ggacgtgtg acgtccatcc acatcagga gcacgagatc  
2341 **gacgccc**g acaccaagt gggcgccgag gagatcacc gggacatccc gaactctcc  
2401 gacgaggtg tggccgacct ggacgagcgc ggatcgtgc gcatcggcgc cgaggtccg  
2461 gacggcaca tctggtcgg caaggtcacc ccgaagggg agaccgagct gacgcccgg  
2521 gagcggctg tcgcgccat cttcggcgag aaggcccgc aggtccgca cacctcgtg  
2581 aaggtgccg acggcgagtc cggcaaggtc atcggatcc ggtgttctc ccgagaggc  
2641 gacgacgagc tgcccggcg ggtcaacgag ctggtccgc tctactggc ccagaagcgc  
2701 aagatctcc acggtgaca gctcggcgc cggcagggca acaagggcgt catcggcaag  
2761 atcctgccg aggaggacat gccgttcta ccggacggca cggcgtgga catcatctg  
2821 aacaccacg gtgtccgag acggatgaac atcggccaga tctggagac ccactgggg  
2881 tgggtggca agtccggtg gaacatcgc ggcaatccc agtggcggt caactgccc  
2941 gaggagctg gccacgcaca gccgaaccag atcgtgtcga caccggtgt cgacggcgc  
3001 aaggaagag agtggcccg catgctgtc tgcacgtgc ccaaccgca cggcaggtc  
3061 atggtgacg gcgacggca ggcggtgct tgcacggcc ggtccgggga cccgttccc  
3121 taccgggta ccgctggcta catgtacatc atgaagctc accacctgt ggacgacaag  
3181 atccacgccc gtccaccgg cccgtactc atgatcacc agcagccgt gggcgtaag  
3241 gcgagttcg gtggccagc cttcgtgag atggagtgt gggccatga ggcctacgg

3301 gcggcgtaga cgctgcagga gctgtgacc atcaagtccg acgacacggg cggccgggtc  
3361 aaggtgtacg aggcgatcgt caagggcgag aacatcccgg agccgggtat ccccgagtcc  
3421 ttcaaggtgt tgctcaagga gctgcagtcg ctgtgcctca acgtcgaggt gctctcctcc  
3481 gacggcgagg ccatcgagct gcgcaaggc gaggacgagg acctggagcg ggccgcggcg  
3541 aacctgggaa tcaactgtc ccgcaacgaa tccgcgtccg tcgaggacct ggcttaa

**Figure 24 Entire rpoB sequence for MAP strain UCF4.**

**Note the A2284C mutation and its position relative further downstream of the 81 bp variable region. Red bold circled positions correspond to mutations that caused an amino acid alteration, and blue bold correspond to silent mutations.**

## 4. DISCUSSION

### 4.1. Purpose

The purpose of our experiment was to characterize MAP's potential for developing RFB and RIF resistance, associate RFB and RIF resistance with mutations in the *rpoB* gene of MAP, and provide an effective protocol for detecting resistant mutations in MAP strains linked to CD. Bacteria such as *M. avium* spp. *avium*, *E. coli*, *H. pylori*, *S. aureus* and *M. kansasii* have laid the foundation for RFB and RIF resistance through mutations in the *rpoB* gene (15,19,25,30,33). Moreover, various strains of the closely related *M. tuberculosis* have set a fine trend for rifamycin resistance, as seen through *rpoB* mutations (1,2,3,4,8,19,20,27,29,41). Our goal was to discover this trend in MAP, and develop an effective method for analyzing RFB and RIF resistance in the bacterium through *rpoB*-based PCR analysis.

### 4.2. Rationale

The overall concept of our research was to develop a method for detecting RIF and RFB resistance in MAP strains to effectively treat CD as well as MAP related infections. In order to thoroughly approach our goal, we established necessary steps to evaluate the level of susceptibility to RIF and RFB in MAP. Therefore, the most effective approach was to perform the following: Identify all MAP isolates through the commonly known IS900 nested PCR reaction. Then investigate *rpoB* sequences in regions commonly known to develop mutations upon RIF resistance. These regions were harbored in those amplified by UCF1/UCF2 and Knight1/Knight2 primers. These regions overlap similar sequences in the *rpoB* gene of *M. tuberculosis* that have displayed mutations upon rifamycin resistance, including the 81 bp region 1276-1356 within

cluster I, as well as a region further upstream in the beginning of *rpoB* (18,19,34).

Consequently, our determinant regions of interest in the *rpoB* gene of MAP were selected based on the available information for closely related bacteria.

Our expected results were to discover no mutations in these regions for susceptible MAP strains. However, upon our recognition of the slight increase in MIC of MAP strain UCF4, we performed additional sequencing to address our unexpected finding and to determine any additional mutations in our highly resistant MAP strains M18 and UCF5-RIF16r. We then discovered a possible rationale for the increase in MIC in strain UCF4 through the detection of a mutation further downstream of our expected regions, suggesting that alternative regions of the beta subunit may influence the interactive stability between RIF and its target.

#### **4.3. An alternative approach**

There are many limitations regarding assay performance with MAP, and these include the bacterium's slow growing nature. To cope with this limitation, we show an alternative approach that may be applied to this bacterium for the analysis RFB and RIF resistance. Provided by our example of using human PBMNC-infected with MAP, we suggest that significant data relevant to genetic resistance to antibiotics may be obtained without the inconvenient time constraint involved with conventional inhibitory tests. For example, analysis of the *rpoB* gene of MAP will indicate the likelihood of susceptibility to RFB and RIF. This information was validated by our in vitro susceptibility tests for using 10 MAP isolates from various sources, which display low MICs for MAP isolates without significant *rpoB* mutations, and higher MICs for MAP isolates with significant *rpoB* mutations.



#### **4.4. Molecular analysis**

Of our 10 MAP isolates, 2 (20%) showed a suspicious indication for RIF resistance, and these were MAP strains 18 and UCF4. MAP strain 18 consisted of a significant *rpoB* mutation, C1367T, which induced an amino acid change in the beta subunit, Thr456 to Ile 456, consequently causing the observed increase in MIC. On the other hand, MAP strain UCF4 contained an *rpoB* mutation further downstream of the 81 bp variable site, and this mutation caused an amino acid alteration Asn762 to His762, resulting in only a slight increase in MIC compared to strain M18. This suggests that the 81 bp region was of upmost significance for the evaluation of highly RIF and RFB resistant MAP strains. Moreover, the difference in the level of susceptibility suggests that this characteristic may vary depending on the location of the amino acid alteration.

#### **4.5. Induced resistance**

Our induced in vitro resistant MAP strain, UCF5-RIF16r, was indicative of RIF resistance after it's observed growth in the presence of 16 ug/ml, and *rpoB* mutation T1442C. The new mutation caused a differential amino acid expression Leu481 to Pro481, and its significance was observed through the association of a higher MIC against RFB and RIF compared to the control. This data, combined with our analysis of MAP strain 18, showed the potential for MAP to evolve resistance to RFB and RIF in vivo and in vitro.

#### **4.6. Blood mixture**

A separate experiment in which we applied our *rpoB*-based protocol on human blood mixed with a specific quantity of MAP. This was accomplished through contaminating normal human blood with  $1 \times 10^3$  CFU's of MAP strain 18, and extracting bacterial DNA directly from the blood mixture. As a result, a sufficient amount

of bacterial DNA was obtained for successful amplification of our regions of interest within *rpoB* (data not shown). The purpose of this approach was to demonstrate the effectiveness of our protocol on CD patient blood.

#### **4.7. Final Comments**

In conclusion, through the application of our protocol on CD patient samples, we may assist in the determination of RFB and RIF susceptible MAP strains for the treatment of CD. Upon the observed in vitro generation of a RFB and RIF resistant MAP strain (UCF5-RIF16r), it is likely that this trend may occur in vivo, as supported with data from MAP strain 18. Furthermore, as RFB is applied more towards the treatment of CD, our protocol will be of utmost significance for the optimization of CD treatment with related antibiotics.

## REFERENCES

1. **Ahmad, S., and E. Mokaddas.** 2005. The occurrence of rare rpoB mutations in rifampicin-resistant clinical Mycobacterium tuberculosis isolates from Kuwait. *Int J Antimicrob Agents.* **26**:205-212.
2. **Aktas, E., R. Durmaz, D. Yang, and Z. Yang.** 2005. Molecular characterization of isoniazid and rifampin resistance of Mycobacterium tuberculosis clinical isolates from Malatya, Turkey. **11**:94-99.
3. **Anthony, R. M., A. R. Schuitema, I. L. Bergval, T. J. Brown, L. Oskam, and P. R. Klatster.** 2005. Acquisition of rifabutin resistance by a rifampicin resistant mutant of Mycobacterium tuberculosis involves an unusual spectrum of mutations and elevated frequency. *Ann Clin Microbiol Antimicrob.* **4**:9.
4. **Bakonyte, D., A. Baranauskaite, J. Cicenaite, A. Sosnovskaja, and P. Stakenas.** 2005. Mutations in the rpoB gene of rifampicin-resistant Mycobacterium tuberculosis clinical isolates from Lithuania. *Int J Tuberc Lung Dis.* **9**:936-938.
5. **Borody, T. J., S. Bilkey, A. R. Wettstein, S. Leis, G. Pang, and S. Tye.** 2007. Anti-mycobacterial therapy in Crohn's disease heals mucosa with longitudinal scars. *Dig Liver Dis.* Epub ahead of print.
6. **Borody, T. J., S. Leis, E. F. Warren, and R. Surace.** 2002. Treatment of severe Crohn's disease using antimycobacterial triple therapy--approaching a cure? *Dig Liver Dis.* **34**:29-38.

7. **Campbell, E. A., N. Korzheva, A. Mustaev, K. Murakami, S. Nair, A. Goldfarb, and S. A. Darst.** 2001. Structural mechanism for rifampicin inhibition of bacterial rna polymerase. *Cell*. **104**:901-912.
8. **Cavusoglu, C., Y. Karaca-Derici, and A. Biligic.** 2004. In-vitro activity of rifabutin against rifampicin-resistant *Mycobacterium tuberculosis* isolates with known rpoB mutations. *Clin Microbiol Infect*. **10**:662-665.
9. **Chamberlin, W., G. Ghobrial, M. Chehtane, and S. A. Naser.** 2007. Successful Treatment of a Crohn's Disease Patient Infected With Bacteremic *Mycobacterium paratuberculosis*. **102**:689-691.
10. **Chamberlin, W., D. Y. Graham, K. Hulten, H. M. El-Zimaity, M. R. Schwartz, S. A. Naser, I. Shafran, and F. A. El-Zaatari.** 2001. Review article: *Mycobacterium avium* subsp. *paratuberculosis* as one cause of Crohn's disease. *Aliment Pharmacol Ther*. **15**:337-346.
11. **Chamberlin, W. M., and S. A. Naser.** 2006. Integrating theories of the etiology of Crohn's disease. On the etiology of Crohn's disease: questioning the hypotheses. *Med Sci Monit*. **12**:RA27-33.
12. **Chiodini, R. J.** 1989. Crohn's disease and the mycobacterioses: a review and comparison of two disease entities. *Clin Microbiol Rev*. **2**:90-117.
13. **Chiodini, R. J., H. J. Van Kruiningen, W. R. Thayer, R. S. Merkal, and J. A. Coutu.** 1984. Possible role of mycobacteria in inflammatory bowel disease. I. An unclassified *Mycobacterium* species isolated from patients with Crohn's disease. *Dig Dis Sci*. **29**:1073-1079.

14. **Gao, A., L. Mutharia, M. Raymond, and J. Odumeru.** 2007. Improved template DNA preparation procedure for detection of *Mycobacterium avium* subsp. paratuberculosis in milk by PCR. Epub ahead of print.
15. **Glocker, E., C. Bogdan, and M. Kist.** 2007. Characterization of rifampicin-resistant clinical *Helicobacter pylori* isolates from Germany. *J. Antimicrob Chemother.* Epub ahead of print.
16. **Grant, I. R.** 2005. Zoonotic potential of *Mycobacterium avium* ssp. paratuberculosis: the current position. *J Appl Microbiol.* **98**:1282-1293.
17. **Gui, G. P., P. R. Thomas, M. L. Tizard, J. Lake, J. D. Sanderson, and J. Hermon-Taylor.** 1997. Two-year-outcomes analysis of Crohn's disease treated with rifabutin and macrolide antibiotics. *J Antimicrob Chemother.* **39**:393-400.
18. **Heep, M., B. Brandstatter, U. Rieger, N. Lehn, E. Richter, S. Rusch-Gerdes, and S. Niemann.** 2001. Frequency of *rpoB* mutations inside and outside the cluster I region in rifampin-resistant clinical *Mycobacterium tuberculosis* isolates. *J Clin Microbiol.* **39**:107-110.
19. **Heep, M., U. Rieger, D. Beck, and N. Lehn.** 2000. Mutations in the beginning of the *rpoB* gene can induce resistance to rifamycins in both *Helicobacter pylori* and *Mycobacterium tuberculosis*. *Antimicrob Agents Chemother.* **44**:1075-1077.
20. **Hermon-Taylor, J.** 2000. Causation of Crohn's disease by *Mycobacterium avium* subspecies paratuberculosis. *Can J Gastroenterol.* **14**:521-539.
21. **Hermon-Taylor, J.** 2001. Protagonist. *Mycobacterium avium* subspecies paratuberculosis is a cause of Crohn's disease. *Gut.* **49**:757-760.

22. **Hermon-Taylor, J.** 2002. Treatment with drugs active against *Mycobacterium avium* subspecies paratuberculosis can heal Crohn's disease: more evidence for a neglected public health tragedy. *Dig Liver Dis.* **34**:9-12.
23. **Hermon-Taylor, J. N. Barnes, C. Clarke, and C. Finlayson.** 1998. *Mycobacterium paratuberculosis* cervical lymphadenitis, followed five years later by terminal ileitis similar to Crohn's disease. *BMJ.* **316**:449-453.
24. **Hetherington, S. V., A. S. Watson, and C. C. Patrick.** 1995. Sequence and analysis of the *rpoB* gene of *Mycobacterium smegmatis*. *Antimicrob Agents Chemother.* **39**:2164-2166.
25. **Jin, D. J., and C. A. Gross.** 1989. Characterization of the pleiotropic phenotypes of rifampin-resistant *rpoB* mutants of *Escherichia coli*. *J Bacteriol.* **171**:5229-5231.
26. **Jou, R., H. Y. Chen, C. Y. Chiang, M. C. Yu, and I. J. Su.** 2005. Genetic diversity of multidrug-resistant *Mycobacterium tuberculosis* isolates and identification of 11 novel *rpoB* alleles in Taiwan. *J Clin Microbiol.* **43**:1390-1394.
27. **Klein, J. L., T. J. Brown, and G. L. French.** 2001. Rifampin resistance in *Mycobacterium kansasii* is associated with *rpoB* mutations. *Antimicrob Agents Chemother.* **45**:3056-3058.
28. **Ma, X., H. Wang, Y. Deng, Z. Liu, Y. Liu, Y. Xu, X. Pan, J. M. Musser, and E. A. Graviss.** 2006. *rpoB* Gene mutations and molecular characterization of rifampin-resistant *Mycobacterium tuberculosis* isolates from Shandong Province, China. *J Clin Microbiol.* **44**:3409-3412.

29. **McCammon, M. T., J. S. Gillette, D. P. Thomas, S. V. Ramaswamy, E. A. Graviss, B. N. Kreiswirth, J. Vijg, and T. N. Quitugua.** 2005. Detection of rpoB mutations associated with rifampin resistance in *Mycobacterium tuberculosis* using denaturing gradient gel electrophoresis. *Antimicrob Agents Chemother.* **49**:2200-2209.
30. **Murphy, C. K., S. Mullin, M. S. Osburne, J. van Duzer, J. Siedlecki, X. Yu, K. Kerstein, M. Cynamon, and D. M. Rothstein.** 2006. In vitro activity of novel rifamycins against rifamycin-resistant *Staphylococcus aureus*. *Antimicrob Agents Chemother.* **50**:827-834.
31. **Naser, S. A, G. Ghobrial, C. Romero, and J. F. Valentine.** 2004. Culture of *Mycobacterium avium* subspecies paratuberculosis from the blood of patients with Crohn's disease. *Lancet.* **364**:1039–1044.
32. **Naser, S. A., I. Shafran, D. Schwartz, F. El-Zaatari, and J. Biggerstaff.** 2002. In situ identification of mycobacteria in Crohn's disease patient tissue using confocal scanning laser microscopy. *Mol Cell Probes.* **16**:41–48.
33. **Obata, S., Z. Zwolska, E. Toyota, K. Kudo, A. Nakamura, T. Sawai, T. Kuratsuji, and T. Kirikae.** 2006. Association of rpoB mutations with rifampicin resistance in *Mycobacterium avium*. *Int J Antimicrob Agents.* **27**:32-39.
34. **Ramaswamy, S., and J. M. Musser.** 1998. Molecular genetic basis of antimicrobial agent resistance in *Mycobacterium tuberculosis*. *Tuberc Lung Dis.* **79**:3-29.
35. **Romero, C., A. Hamdi, J. F. Valentine, and S. A. Naser.** 2005. Evaluation of surgical tissue from patients with Crohn's disease for the presence of *Mycobacterium avium* subspecies paratuberculosis DNA by in situ hybridization and nested polymerase chain reaction. *Inflamm Bowel Dis.* **11**:116-125.

36. **Shafran, I., L. Kugler, F. A. El-Zaatari, S. A. Naser, and J. Sandoval.** 2002. Open clinical trial of rifabutin and clarithromycin therapy in Crohn's disease. *Dig Liver Dis.* **34**:22-28.
37. **Schwartz, D., I. Shafran, C. Romero, C. Piromalli, J. Biggerstaff, N. Naser, W. Chamberlin, and S. A. Naser.** 2000. Use of short-term culture for identification of *Mycobacterium avium* subsp. *paratuberculosis* in tissue from Crohn's disease patients. *Clin Microbiol Infect.* **6**:303-307.
38. **Thompson, D. E.** 1994. The role of mycobacteria in Crohn's disease. *J. Med. Microbiol.* **41**:74–94.
39. **Williams, S. L., N. B. Harris, and R. G. Barletta.** 1999. Development of a firefly luciferase-based assay for determining antimicrobial susceptibility of *Mycobacterium avium* subsp. *paratuberculosis*. *J Clin Microbiol.* **37**:304-309.
40. **Xu, M., Y. N. Zhou, B. P. Goldstein, and D. J. Jin.** 2005. Cross-resistance of *Escherichia coli* RNA polymerases conferring rifampin resistance to different antibiotics. *J Bacteriol.* **187**:2783-2792.
41. **Yuen, L. K., D. Leslie, and P. J. Coloe.** 1999. Bacteriological and molecular analysis of rifampin-resistant *Mycobacterium tuberculosis* strains isolated in Australia. *J Clin Microbiol.* **37**:3844-3850.
42. **Zhanel, G. G., M. H. Saunders, J. N. Wolfe, D. J. Hoban, J. A. Karlowsky, and A. M. Kabani.** 1998. Comparison of CO<sub>2</sub> generation (BACTEC) and viable-count methods to determine the postantibiotic effect of antimycobacterial agents against *Mycobacterium avium* complex. *Antimicrob Agents Chemother.* **42**:184-187.



43. **Zubrick, B., and C. Czuprynski.** 1987. Ingestion and intracellular growth of *Mycobacterium paratuberculosis* within bovine blood monocytes and monocyte-derived macrophages. *Infect Immun* **55**:1588–1593.